Reversible Charge Trapping in Bis-Carbazole-Diimide Redox Polymers with Complete Luminescence Quenching Enabling Nondestructive Read-Out by Resonance Raman Spectroscopy

Kortekaas, Luuk; Lancia, Federico; Steen, Jorn D; Browne, Wesley R

Published in:
The Journal of Physical Chemistry. C: Nanomaterials and Interfaces

DOI:
10.1021/acs.jpcc.7b04288

Publication date:
2017

THE JOURNAL OF PHYSICAL CHEMISTRY C

Article

pubs.acs.org/JPCC

Reversible Charge Trapping in Bis-Carbazole-Diimide Redox Polymers with Complete Luminescence Quenching Enabling Nondestructive Read-Out by Resonance Raman Spectroscopy

Luuk Kortekaas, Federico Lancia, Jorn D. Steen, and Wesley R. Browne*

Stratingh Institute for Chemistry, University of Groningen, Nijenborgh 4, 9747AG Groningen, The Netherlands

Supporting Information

ABSTRACT: The coupling of substituted carbazole compounds through carbon−carbon bond formation upon one-electron oxidation is shown to be a highly versatile approach to the formation of redox polymer films. Although the polymerization of single carbazole units has been proposed earlier, we show that by tethering pairs of carbazoles double sequential dimerization allows for facile formation of redox polymer films with fine control over film thickness. We show that the design of the monomers and in particular the bridging units is key to polymer formation, with the diaminobenzene motif proving advantageous, in terms of the matching to the redox potentials of the monomer and polymer film and thereby avoiding limitations in film thickness (autoinsulation), but introduces unacceptable instability due to the intrinsic redox activity of this moiety. The use of a diimide protecting group both avoids complications due to *p*-diamino-benzene redox chemistry and provides for a redox polymer in which the photoluminescence of the bis-carbazole moiety can be switched reversibly (on/off) with redox control. The monomer design approach is versatile enabling facile incorporation of additional functional units, such as naphthalene. Here we show that a multicomponent carbazole/naphthalene containing monomer (**APCNDI**) can form redox polymer films showing both p- and n- conductivity under ambient conditions and allows access to five distinct redox states, and a complex electrochromic response covering the whole of the UV/vis−NIR spectral region. The highly effective quenching of the photoluminescence of both components in poly-**APCNDI** enables detailed characterization of the redox polymer films. The poly-**APCNDI** films show extensive charge trapping, which can be read out spectroscopically in the case of films and is characterized as kinetic rather than chemical in origin on the basis of UV/vis−NIR absorption and resonance Raman spectroscopic analyses. The strong resonantly enhanced Raman scattering for the various oxidized and reduced states of **APCNDI** enables nondestructive "read-out" of the state of the polymer, including that in which charges are trapped kinetically at the surface, making poly-**APCNDI** highly suitable for application as a component in organic nonvolatile memory devices.

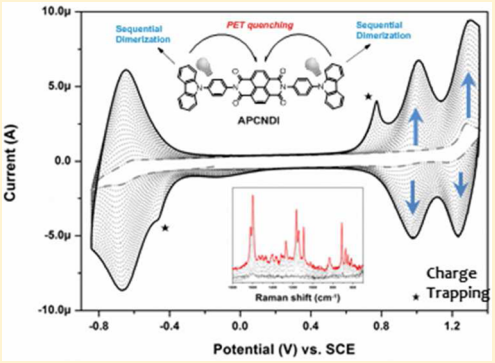

INTRODUCTION

Smart (stimuli responsive) surfaces[1] are attracting increasing attention,[2−4] not least in the field of molecular electronics,[5] due to the opportunities presented by redox switching in rapid localized control of physical and optical properties. Electrochromism, the inducing of reversible color changes by application of a voltage, was first observed in inorganic semiconductors.[6] The later discovery of organic conducting and redox polymers has enabled fine control of HOMO−LUMO band-gaps and hence optical properties as well as their facile processing and application to foldable devices. D−A−D (donor−acceptor−donor) oligoimides in particular have seen application already in high-performance nonvolatile memory devices,[7−16] logic gates,[17] and nonlinear optical materials.[18,19] Intra- and intermolecular interactions in such multicomponent systems often alter the functionality of their individual components,[20,21] which can provide opportunities in their application.

Carbazole and its derivatives have been widely studied for their various physical and electronic properties, the most studied of which, poly(*N*-vinylcarbazole), was the first nitrogen heterocycle containing polymer to show hole transport properties.[22] The discovery of the optical and electrical properties of carbazole containing polymers and oligomers has stimulated their application in areas as diverse as organic light emitting diodes (OLEDs) and organic-thin film transistors,[23−25] organic solar cells,[26−28] and sensors.[29]

Carbazole is often modified with a moiety to allow for incorporation in a polymer, e.g., with vinyl groups[30,31] or through Suzuki coupling,[32] since although the ability of N-substituted carbazoles to undergo polymerization has been proposed, Karon and Lapkowski concluded, in their recent review, that oxidation of N-substituted carbazoles leads mainly to dimers as a consequence of charge delocalization in the 3−3′ dimer.[33] Indeed, Siove and co-workers showed that a monomer in which two carbazole units are tethered by an N-substituted

Received: May 5, 2017
Revised: June 12, 2017
Published: June 12, 2017

DOI: 10.1021/acs.jpcc.7b04288
J. Phys. Chem. C 2017, 121, 14688−14702

Scheme 1. ECCE Mechanism for Sequential Dimerization of Alkyl *N,N*-Coupled Bisindolines and Related Compounds[34,39]

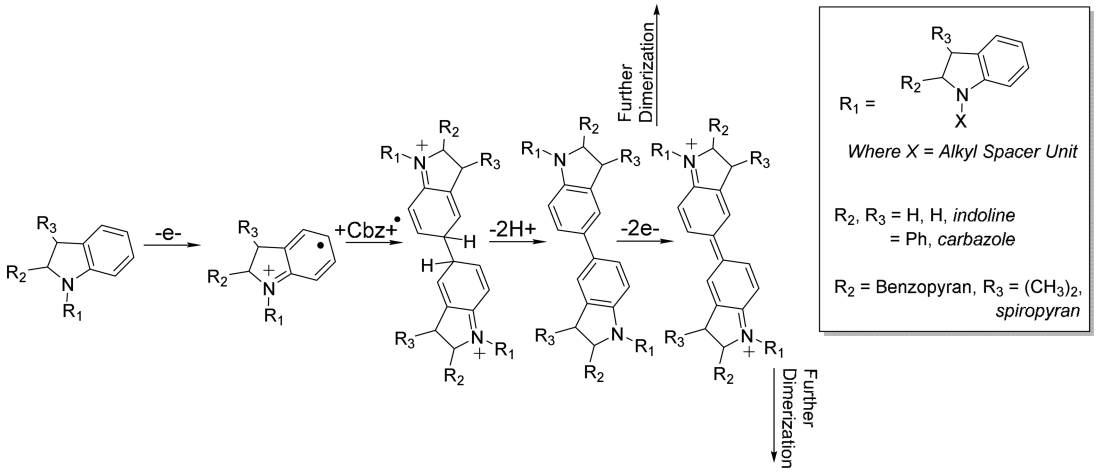

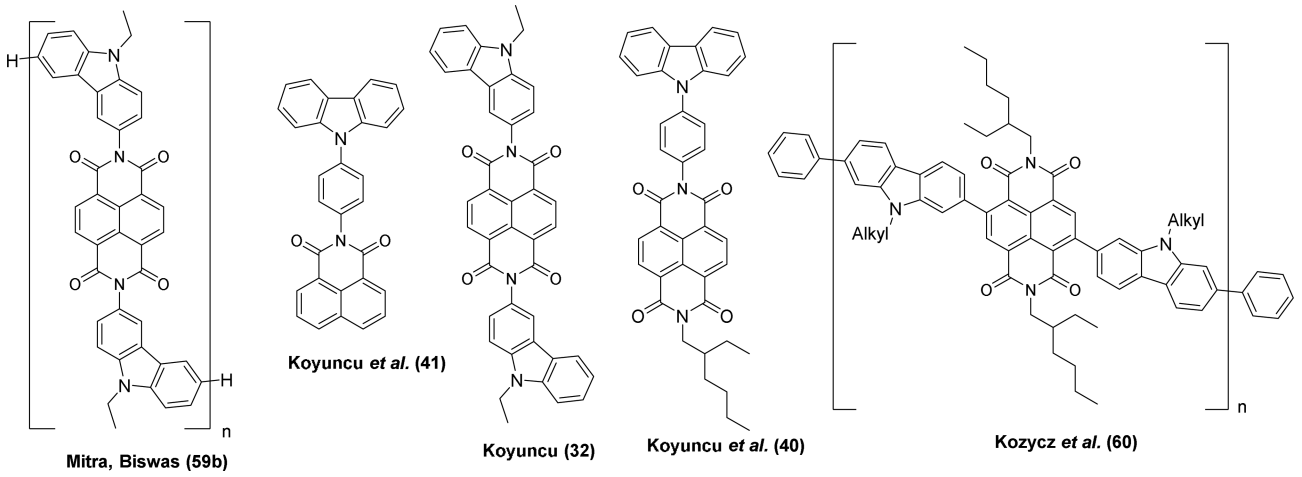

Figure 1. Approaches toward carbazole and naphthalene derived Donor−Acceptor (polymer) systems.

alkyl spacer merely leads to sequential dimerization upon chemical oxidation to form a polymer that could be spin-cast on electrodes.[34] The C−C coupling para to the nitrogen upon (electro)oxidation[24−26] via a 4 electron ECCE process is analogous to the dimerization of indoline derivatives[35] and *N,N*-dialkyl substituted anilines,[36−38] which occur readily. Moreover, direct coupling of two of such moieties covalently via the amine group results in chain-growth elongation of the bisindoline scaffold (Scheme 1) with each unit coupling to another molecule.[39]

Koyuncu et al. reported a carbazole coupled to either perylene[40] or naphthalimide[41] to form energy donor/acceptor (D−A) systems, which can be immobilized by electrochemical coupling of the carbazole units. The films formed show moderate quenching of the fluorescence of both donor and acceptor in the dyads but almost complete quenching of photoluminescence in the films formed electrochemically (Figure 1). The use of only a single carbazole unit in this system, however, requires that each carbazole unit couples to two others in order to form a polymer backbone with pendent naphtal- and perylene-imide units. However, the steric overcrowding expected in the system reported by Koyuncu et al., the stability of the initially formed bis-carbazole dication (which is present at the potentials required for oxidation of monomer), and the poor mechanical stability of the films formed, indicate that dimerization rather than polymerization occurred, with insolubility being the primary driving force for immobilization on the electrodes used. The choice of spacer unit between the carbazole and perylene/naphtalimide (Scheme 1) has a pronounced effect on the efficiency of carbazole−carbazole coupling and the final structure of the films formed.

The spacer unit, in such systems, plays an important role in determining the overall function of the systems. Earlier studies on compounds in which a functional unit, such as a dithienylethene photochromic switch, was tethered to a pair of electrodimerizable/polymerizable units showed that the introduction of a phenyl spacer aids the polymerization process and improves the retention of the functionality of the photoswitchable moiety.[42−44] Koyuncu et al. took a similar approach in which carbazole units are attached directly at their 3-position to both ends of a naphthalene diimide, enabling polymerization through sequential dimerization (Figure 1).[32] With this approach, however, only partial quenching of photoluminescence was observed, ascribed in part due to perturbation of the properties of the carbazole by direct attachment of the diimide unit to it.

1,4,5,8-Naphtalene diimides (NDIs) are chemically robust chromophores which have seen widespread application over the last decades in supramolecular systems such as rotaxanes,[45,46]

DOI: 10.1021/acs.jpcc.7b04288
J. Phys. Chem. C 2017, 121, 14688−14702

catenanes,[47,48] nanotubes,[49] ion channels,[50] foldamers,[51] and synthetic photosystems.[52] Their tendency to self-organize both at the solid state and in solution due to their planarity and to engage in $\pi\pi$ stacking has made them appealing to supramolecular chemistry as they can form or be incorporated readily within supramolecular assemblies. Furthermore, the electronic properties of NDI have found application in sensing and in multicomponent systems in which energy and electron transfer processes are utilized. For example, Takenaka et al. have employed an NDI bearing redox-active ferrocenyl moieties to discriminate between double stranded DNA and single stranded DNA electrochemically.[53] The radical monoanionic form of NDI is readily accessible by chemical and electrochemical reduction,[54] and its electron deficiency in its neutral state favors interaction with electron rich species and anions as highlighted elegantly by Matile et al. in their study of charge transfer (anion-π interactions) and transport between substituted NDI monomers and nanorods with a variety of anions.[55] More recently, Saha et al. reported light-gated electron transfer from anions to aryl substituted NDI.[56,57]

The wider range of applications that can be realized makes the combination of carbazole and NDI in an electrochromic polymer film highly appealing.[58,59] Several approaches toward this goal have been reported to date, making use of various carbazole structures and naphthalene derivatives (Figure 1). Kozycz and co-workers observed quenching of the emission at 700 nm in a D−A carbazole−naphthalene imide polymer obtained through chemical coupling.[60] A drawback of the latter approach is the synthetic effort of chemical coupling, as well as the risk of presence of residual palladium, which limits the range of applications. Lav et al. utilized the propensity of tethered carbazoles to dimerize, forming numerous cross-links through sequential electrodimerization in an oligomer containing carbazole side chains.[61] The key challenge in forming robust redox polymers based on the combination of NDI and carbazole is to achieve polymerization rather than dimerization and to avoid other electrochemically induced reactions.

Here, we report the synthesis and characterization of amino-phenyl carbazole cyclohexane diimide (**APCCDI**), Figure 2,

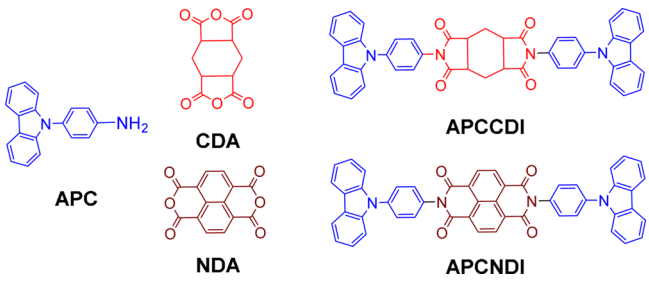

Figure 2. Structure of amino-phenyl carbazole (**APC**), cyclohexane dianhydride (**CDA**), and amino-phenyl carbazole cyclohexane diimide (**APCCDI**), naphthalene dianhydride (**NDA**), and amino-phenyl carbazole naphthalene diimide (**APCNDI**).

and its oxidative electropolymerization on a range of electrode materials under ambient conditions, i.e., without need for strong Lewis acids or inert conditions. The optical and electrochemical properties of the monomer and redox-active polymer films are characterized by UV/vis, FTIR and emission spectroscopy, and cyclic voltammetry.

In addition, two carbazole compounds were prepared for modeling of the oxidative coupling and the impact of the functional groups present in the multicomponent systems on electrochemical stability (Figure 3 and Scheme 2). We show that while the diimide unit performs well under electrochemical conditions, the use of a simpler *N*-aryl amide linkage **D1** shows instability due to the quinoidal character of the oxidized *p*-diamino linker, with decomposition competing with carbazole-carbazole coupling.

Model compounds such as the benzoate based **D2**, however, showed the expected spectroscopic properties of the carbazole dimers after oxidative electrolysis, with a slight red-shift in both the UV/vis absorption and fluorescence spectra. The model monomer (**I1**) and dimer (**I2**) of **APCCDI**, with a single instead of double diimide, provide insight into its properties in the monomeric and polymeric form.

The electrochemical performance of the phenyl carbazole unit, linked through an imide (i.e., as in **APCCDI**), was built upon in a more complex system in which an NDI unit is coupled via imides to two carbazole units to form **APCNDI** (Figure 2) and access the reductive electrochemistry and symmetric rigid structure of NDI in multifunctional polymer films. We show that complete quenching of the photoluminescence of both NDI and bis-carbazole is achieved, which enables the study of the polymer films formed, and assignment of charge trapping as kinetic or thermodynamic (vide infra), using multiwavelength resonance Raman microspectroscopy under electrochemical control. The **APCNDI** polymer films formed show reductive and oxidative electrochromism and selective enhancement of Raman bands of the various accessible redox states. We show that oxidative and reductive kinetic charge trapping can be achieved in thicker films and can be "read out" in poly-**APCNDI** by resonance Raman spectroscopy nondestructively, providing for applications in nonvolatile memory.

EXPERIMENTAL SECTION

Materials. Reagent grade carbazole, *p*-bromonitrobenzene, copper iodide, 1,10-phenantroline, potassium carbonate, hydrazine monohydrate, pyridine, acetic anhydride, cesium carbonate, palladium on charcoal, tetrabutyl ammonium hexafluorophosphate ($TBAPF_6$), $FeCl_3$, 4-iodoaniline, 4-iodobenzoic acid, Cu_2O, and 1,4,5,8-naphthalenetetracarboxylic dianhydride were purchased from Sigma-Aldrich and were used as-received. Reagent grade 1,2-cyclohexane anhydride and 1,2,4,5-cyclohexane dianhyride were purchased from TCI Co., Ltd. and used as-received. Amino-phenyl carbazole (**APC**) was stored as its HCl salt (Supporting Information, SI), and liberated before use. Compound **D1** is the precursor to the **APC**·HCl salt. Compound **D2** was synthesized through esterification of *p*-iodobenzoic acid followed by cuprous oxide mediated carbazole coupling (SI). Details of the synthesis and characterization of **APCCDI** and **APCNDI** are provided as SI (Figures S1−S18).

UV/vis absorption spectroscopy, electrochemistry, in situ UV/vis absorption, and resonance Raman spectroelectrochemical experiments were conducted in spectroscopic (UVASOL) grade dichloromethane (Merck).

Physical Methods. ^1H NMR and ^{13}C NMR spectra were obtained on a Varian Mercury Plus 399.93 MHz spectrometer. Chemical shifts are reported in ppm (δ), coupling constants in Hz, multiplicity is noted as follows: s = singlet, d = doublet, t = triplet, m = multiplet. Chemical shifts are with respect to tetramethylsilane and referenced to residual solvent (either $CHCl_3$ or DMSO-d_5) signals. UV/vis absorption spectra were

DOI: 10.1021/acs.jpcc.7b04288
J. Phys. Chem. C 2017, 121, 14688−14702

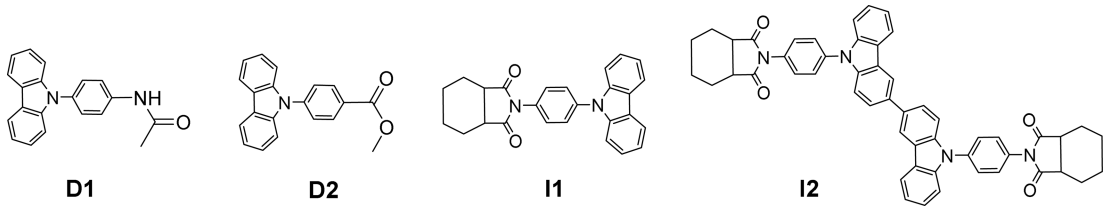

Figure 3. Model compounds used to study carbazole oxidative dimerization, *N*-(*p*-carbazole phenyl)acetamide (**D1**), and methyl *p*-carbazole benzoate (**D2**), amino-phenyl carbazole cyclohexane imide (**A1**), amino-phenyl carbazole cyclohexane imide (**I1**), and its dimer obtained by chemical oxidation (**I2**).

Scheme 2. One Electron Oxidation of Bis-Aminophenyl Modified Carbazole is Centered on the Carbazole Unit but is Expected to Have Significant Contribution from Resonance Structures Involving the Protected Bis-Aminophenyl Unit, Exposing It to Competing Hydrolysis Reactions

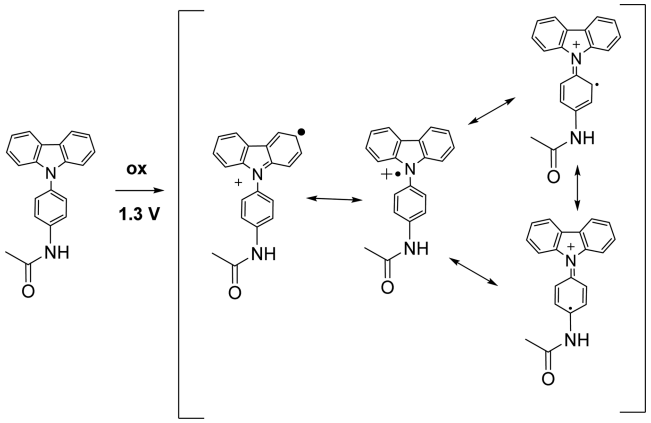

recorded on an Analytik Jena Specord 600 in concentrations ranging from 30 to 60 μM in dichloromethane. In situ UV/vis and vis−NIR absorption spectra, obtained using a quartz cuvette as electrochemical cell with a poly-**APCNDI** modified ITO working electrode, were recorded on an Analytik Jena Specord 600 and a JASCO FT/IR-4600, respectively. Spectra were referenced to a bare ITO coated glass slide in 0.1 M $TBAPF_6$ in dichloromethane and solutions with and without **APCNDI**-monomer were exchanged by syringe to maintain the consistency of the optical path. Electrochemical data were obtained using a CHI760B electrochemical workstation (CH Instruments), all potentials are quoted with respect to the SCE and a sweep rate of 0.1 V s^{-1} was employed unless stated otherwise. A three electrode arrangement was employed with a glassy carbon (diameter 3 mm), platinum (diameter 1.5 mm), or gold (dia 1.5 mm) disc working electrode, a Ag/AgCl wire reference and a platinum wire counter electrode, under argon purge when scanning to negative potentials (<−0.2 V vs SCE). For bulk electrolysis, a rectangular reticulated vitreous carbon (RVC) electrode from ERG Materials & Aerospace Corporation, Oakland, CA, was employed as working electrode. Emission spectra were obtained using a Andor Newton 970-BV EMCCD (operated in CCD mode) camera mounted to a shamrock163 spectrograph with a 300 l/mm grating blazed at 300 nm fiber coupled to a THORLABS cuvette holder (for solutions) or a Nikon TE-Eclipse inverted microscope for modified electrodes. Excitation at 300 and 365 nm used Fiber coupled LEDs (thorlabs). FTIR spectra were recorded on a PerkinElmer FTIR Spectrum 400 equipped with a UATR attachment. Mass spectra were recorded on a MALDI TOF Voyager DE-Pro by Applied Biosystems and a Xevo G2 Q-TOF DART by Waters Corporation. In situ Resonance Raman spectroelectrochemistry was performed following electropolymerization on a platinum disc working electrode by repeated cyclic voltammetry, followed by washing of the polymer modified electrode with dichloromethane and immersion in dichloromethane with 0.1 M $TBAPF_6$. In situ measurements were performed on a PerkinElmer Raman station with excitation at 785 nm using a quartz cuvette as electrochemical cell. Raman spectra were recorded at λ_{exc} 266 nm (0.6 mW at sample, obtained by frequency doubling of the 532 nm output of a DPSS laser using a Newport WaveTrain) and 355 nm (10 mW at sample, Cobolt lasers) in 135° and 180° backscattering mode, respectively. Raman scattering was collimated and subsequently refocused by a pair of 25 mm planoconvex lens (7.5 and 15 mm focal lengths, respectively) into a Shamrock500 spectrograph (Andor technology) with a 2400 l/mm grating blazed at 300 nm onto a iDus-420-BU2 CCD (Andor Technology). Spectra were acquired and processed using Andor Solis and PerkinElmer Spectrum 10.0, respectively. Fluorescence spectra were recorded using quartz cuvettes containing 5 nM solutions of analyte in dicholoromethane with excitation provided by a 75 W xenon lamp coupled to a Zolix 150 mm monochromator and to a qpod (Quantum Northwest) temperature controlled cuvette holder. The emission was collected at 90° through a fiber optic connected to an iDus-420-OE CCD camera (Andor Techology).

RESULTS AND DISCUSSION

UV/vis Absorbance and Emission Spectroscopy of D1 and D2. Although the polymerization of carbazole derivatives has been proposed elsewhere,[62,63] the propensity of *N*-phenyl carbazole derivatives to undergo oxidative C−C bond formation to form dimers rather than other electrochemical reactions[33] was investigated in the model compounds **D1** and compound **D2** (Figure 3). Both **D1** and **D2** are comprised of an aryl N-substituted carbazole unit, however, **D2** does not bear the *p*-bis-amino motif of **D1**. Although the cyclic voltammetry of **D1** (Figure S6) indicates a propensity to undergo dimerization by C−C coupling of the carbazole units, preparative electrolysis resulted in a general decrease in UV absorbance and completely loss in emission intensity (Figure 4 upper). In contrast, cyclic voltammetry (Figure S7) and preparative oxidative electrolysis of solutions of **D2** resulted in a minor broadening in the UV/vis absorbance spectrum and a red shift of the emission spectrum consistent with formation of a *bis*-carbazole (Figure 4 lower). In both cases, there was no indication of formation of polymer films at the working electrodes. The greater stability, with regard to oxidation, of **D2** indicates that for **D1** the quinoidal character of the *p*-bis-amino

DOI: 10.1021/acs.jpcc.7b04288
J. Phys. Chem. C 2017, 121, 14688−14702

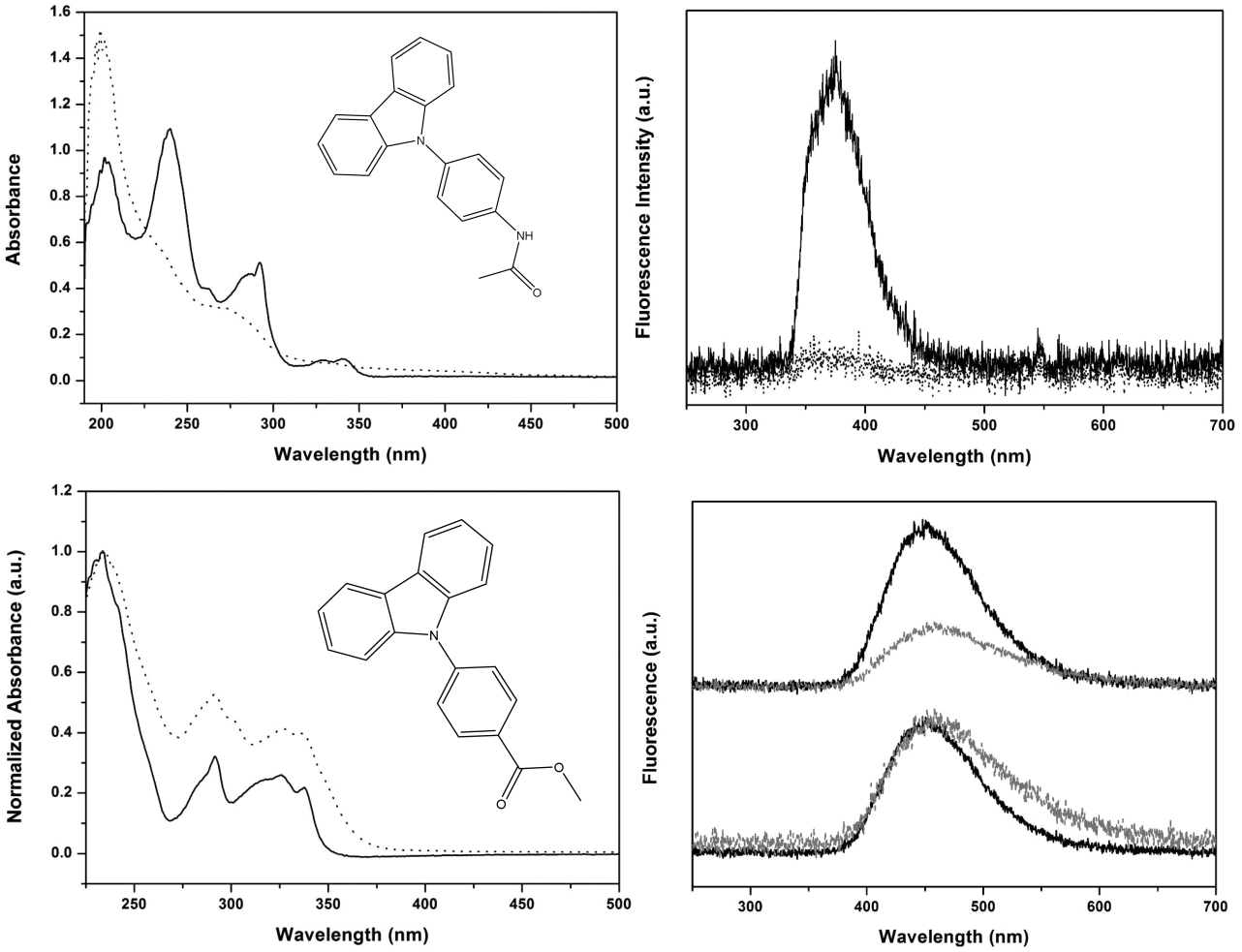

Figure 4. (Top left) UV/vis absorbance and (top right, λ_{exc} 300 nm) emission spectra of **D1** before (black) and after preparative anodic electrolysis (black dotted) at 1.2 V for 15 min. (Bottom left) UV/vis absorbance and (bottom right, λ_{exc} 300 nm) emission spectra of **D2** in dichloromethane (solid line) before and after preparative anodic electrolysis (dotted line) at 1.2 V for 1 h. (Bottom right) Emission spectra showing change in relative emission intensity and normalized spectra. Conditions: in dichloromethane with 0.1 M $TBAPF_6$ with a carbon mesh working, SCE reference and platinum counter electrode.

motif is important and reaction of this moiety after oxidation may compete effectively with carbazole dimerization.

Compound **I1**, prepared from **APC** (aminophenyl carbazole) by reaction with cyclohexyl-1,2-dicarboxy anhydride was dimerized by chemical oxidation[64,65] to yield model compound **I2**. Dimerization of **I1** to form **I2** results in broadening of the UV absorption bands and a redshift in the emission (Figure 5), as observed for **D1**/**D2**.

The retention of the absorption and emission properties upon oxidative coupling of **I1** to form **I2** indicates that the diimide connection prevents involvement of the *p*-bis-amino motif in the redox chemistry of the compounds. Hence the structure **APCCDI**, prepared analogously to **I1** (see SI), was expected to undergo sequential oxidative dimerization of the imide-linked phenyl carbazoles (Scheme 1).

Indeed the cyclic voltammetry of **APCCDI** is as expected for an indole containing compound,[35−37] i.e., a 4-electron ECCE process resulting in dimerization via aryl−aryl coupling (Figure 6). Two carbazole radical cations, formed an electrochemically, couple and undergo double deprotonation to rearomatize. This process is followed by immediate oxidation to the product's doubly cationic state at the applied potential, with two new redox waves on the return cycle assigned to the first and second reductions of the $[\text{bis-carbazole}]^{2+}$ units formed.

In contrast to compound **I1**, however, dimerization leaves two carbazole units connected via the diimide bridges, which can undergo subsequent coupling to other carbazole units and hence stepwise chain elongation. The oligomers are insoluble and deposit on the electrode surface readily leading to the buildup of a redox polymer manifested in the steady increase in current ($I_{p,a}$ and $I_{p,c}$) of the redox waves of the bis-carbazole unit (Figure 7). Importantly the oxidation potential of **APCCDI** is close to that of the second oxidation of the bis-carbazole unit formed and hence film growth is not limited by lack of conductivity at the onset potential for polymerization. The voltammetry of polymer modified electrode in monomer free solution shows the redox waves of poly-**APCCDI**, indicating that the polymer is well adhered to the electrode surface and is not affected substantially by the presence adventitious water or oxygen. Films from poly-**APCCDI** were formed readily at glassy carbon, platinum, and ITO on glass slide electrodes indicating that surface polymer interactions are not especially important in achieving adhesion, but instead that solubility is the primary driving force.

DOI: 10.1021/acs.jpcc.7b04288
J. Phys. Chem. C 2017, 121, 14688−14702

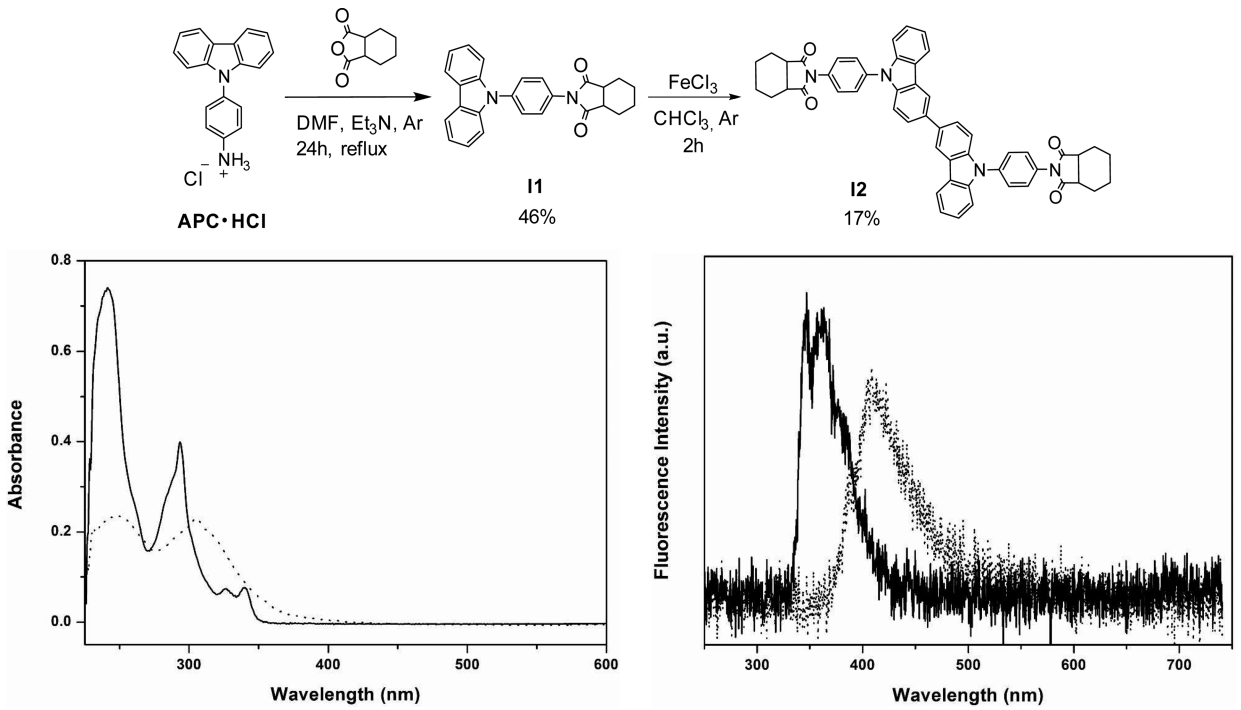

Figure 5. Synthesis of **I1** and **I2** from the **APC**·HCl salt and (left) UV/vis absorbance and (right) emission spectra of **I1** (solid line) and **I2** (dotted line) in dichloromethane.

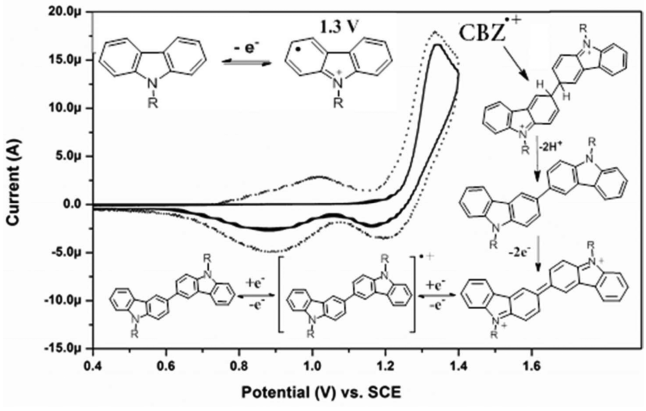

Figure 6. Oxidative cyclic voltammetry of **APCCDI** (0.1 mM) in dichloromethane (SCE reference and platinum counter electrode, 0.1 M $TBAPF_6$, scan rate 0.1 V s^{-1}) at a Au working electrode (d = 3 mm), and the corresponding mechanism of the electrochemical dimerization. Initial cycle (thick line), second cycle (dotted line).

Electrochemical Modulation of poly-APCCDI Fluorescence. The fluorescence of poly-**APCCDI** was expected to be similar to that of **I2**, however, immobilization in a polymer film at a, e.g., Au, macroelectrode could result in emission quenching due to intermolecular interactions. The emission of poly-**APCCDI**, excited at λ_{exc} 365 nm, was less well-defined (broader) than that of **I2**, but is nevertheless, together with its slight red-shift, typical for the bis-carbazole motif.[66] Oxidation resulted in complete quenching of photoluminescence with full recovery upon reduction to the neutral state (Figure 8). Monitoring of photoluminescence switching during multiple potential steps shows that relatively rapid switching on and off of polymer emission with a response time that indicated charge diffusion was limiting (vide infra).

Multiresponsive Bis-Carbazole Based Redox Polymer Films Incorporating Naphthalene Diimide. The versatility of the bis-imide bridging motif in **APCCDI**, prompted the incorporation of a naphthalene unit to increase functionality and the preparation of **APCNDI** (for details of synthesis and characterization, see SI, and Figure S16). The absorption spectrum of **APCNDI** shows the characteristic vibronic progression ($\pi-\pi^*$ transition) of the naphthalene diimide with maxima at 320, 340, 360, and 380 nm, which overlap with the lowest $\pi-\pi^*$ transitions of the carbazole moiety (Figure 9). The absorption bands are shifted bathochromically compared with the precursor 1,4,5,8-naphthalenetetracarboxylic dianhydride (NDA).[54] At λ_{exc} 266 nm, the emission spectrum of an equimolar mixture of NDA and *p*-CMBz is dominated by carbazole emission (Figure 9),[67,68] consistent with the large difference in molar absorptivity of the components. At λ_{exc} 355 nm, the emission from both components is similar in intensity. In contrast, the **APCNDI** shows essentially no emission upon excitation at either wavelength with only Raman scattering from solvent observed, indicating highly efficient emission quenching, considering the components redox chemistry (vide infra), by photoinduced electron transfer (PET) from the carbazole to the naphthalene moieties (Scheme 3). Importantly, the extent of quenching seen in these data confirm the absence of unreacted NDA and the carbazole precursor in **APCNDI** and contrasts sharply with that observed for the naphthalene bis-carbazole system reported by Koyuncu, in which emission was observed and even increased 3-fold with subsequent electropolymerization.[32]

Resonance Raman Spectroscopy of APCNDI. The strong blue emission of both carbazole and naphthalene diimide precludes the application of resonance Raman spectroscopy with excitation in the 250−400 nm range (vide supra and Figure S19). The highly efficient photoinduced electron transfer quenching from the carbazole to the NDI

DOI: 10.1021/acs.jpcc.7b04288
J. Phys. Chem. C 2017, 121, 14688−14702

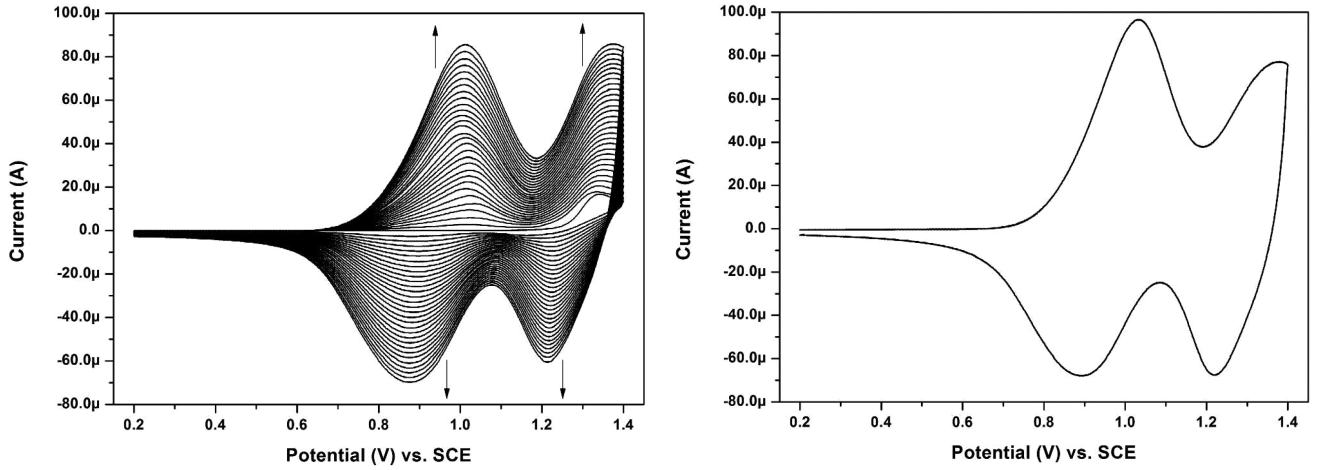

Figure 7. (Left) Cyclic voltammetry of **APCCDI** (0.1 mM) at a Au electrode (d = 3 mm), and (right) cyclic voltammetry of the poly-**APCCDI** modified electrode in a monomer free solution. In dichloromethane, 0.1 M $TBAPF_6$, Pt counter, and SCE working electrode, scan rate 0.1 V s^{-1}), final surface coverage is estimated to be 2.4 × 10^{-8} mol cm^{-2} on the basis of the anodic charge passed.

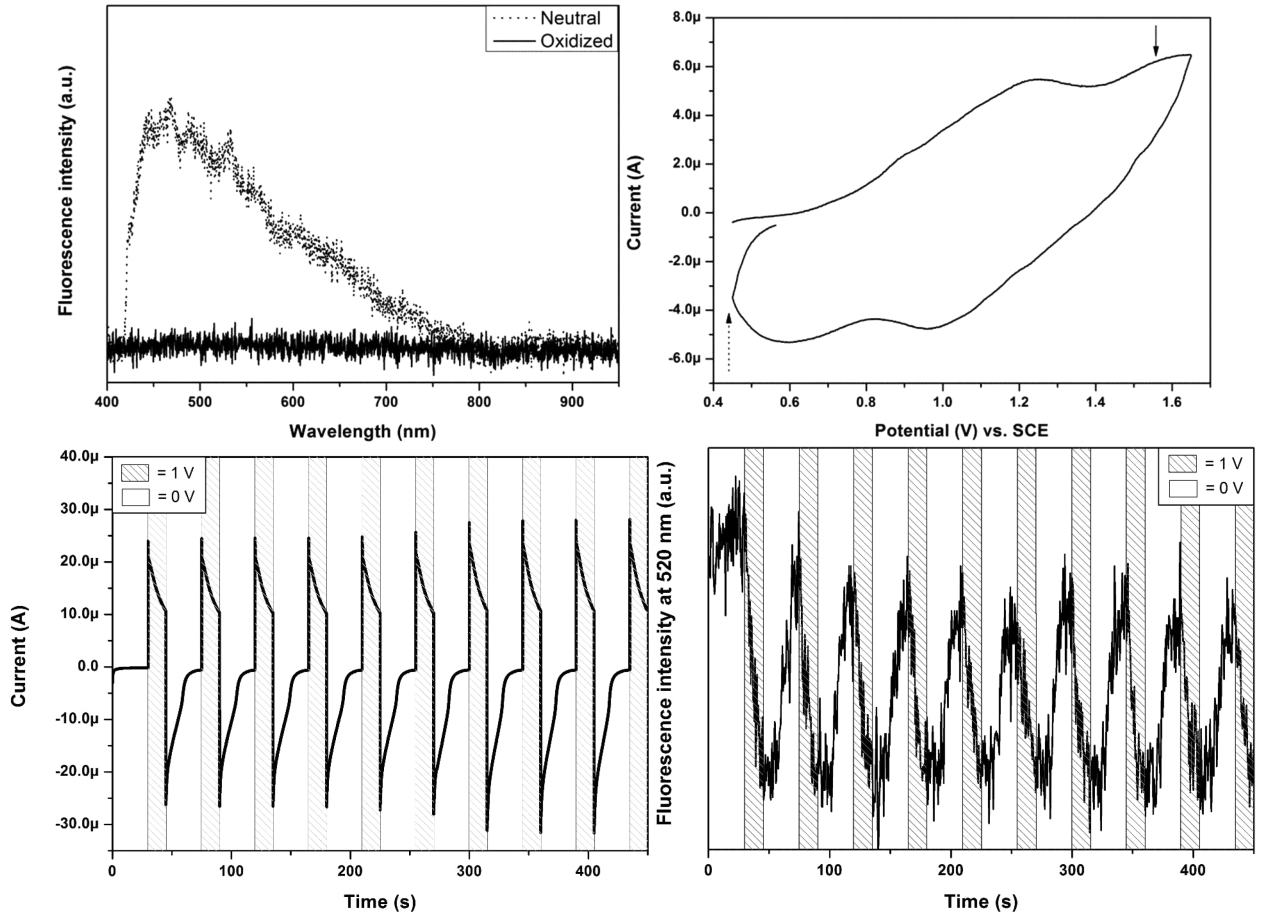

Figure 8. (upper left) In situ photoluminescence (λ_{exc} = 365 nm) of poly-**APCCDI** and (upper right) the corresponding cyclic voltammetry of the poly-**APCCDI** modified Au electrode in dichloromethane (0.1 V s^{-1}, 0.1 M $TBAPF_6$). Multistep potential switching cycles with alternating polarization at 0 V for 30 s and 1 V for 15 s. (lower left) current response upon switching the potential and (lower right) the corresponding photoluminescence at 520 nm (λ_{exc} 365 nm). SCE reference and platinum counter electrodes.

moiety observed in **APCNDI**, however, allows resonance Raman spectra to be recorded in dilute solutions at λ_{exc} 266 and 355 nm (Figure 10). Enhancement of Raman bands at 1625 and 1237 cm^{-1} corresponding to those observed in the Raman spectra of carbazole is seen at λ_{exc} 266 nm and assigned to aromatic ring stretch and C−N stretch vibrations, respectively, of the carbazole moiety only (since the NDI unit does not absorb significantly at this wavelength and indeed NDA shows only very weak resonance enhancement at λ_{exc} 266 nm, Figure S20). The carbazole in plane bending modes at 1178 and 1019 cm^{-1}, and out of plane bending mode at 705 cm^{-1} were also observed. Resonance enhancement of both the naphthalene

DOI: 10.1021/acs.jpcc.7b04288
J. Phys. Chem. C 2017, 121, 14688−14702

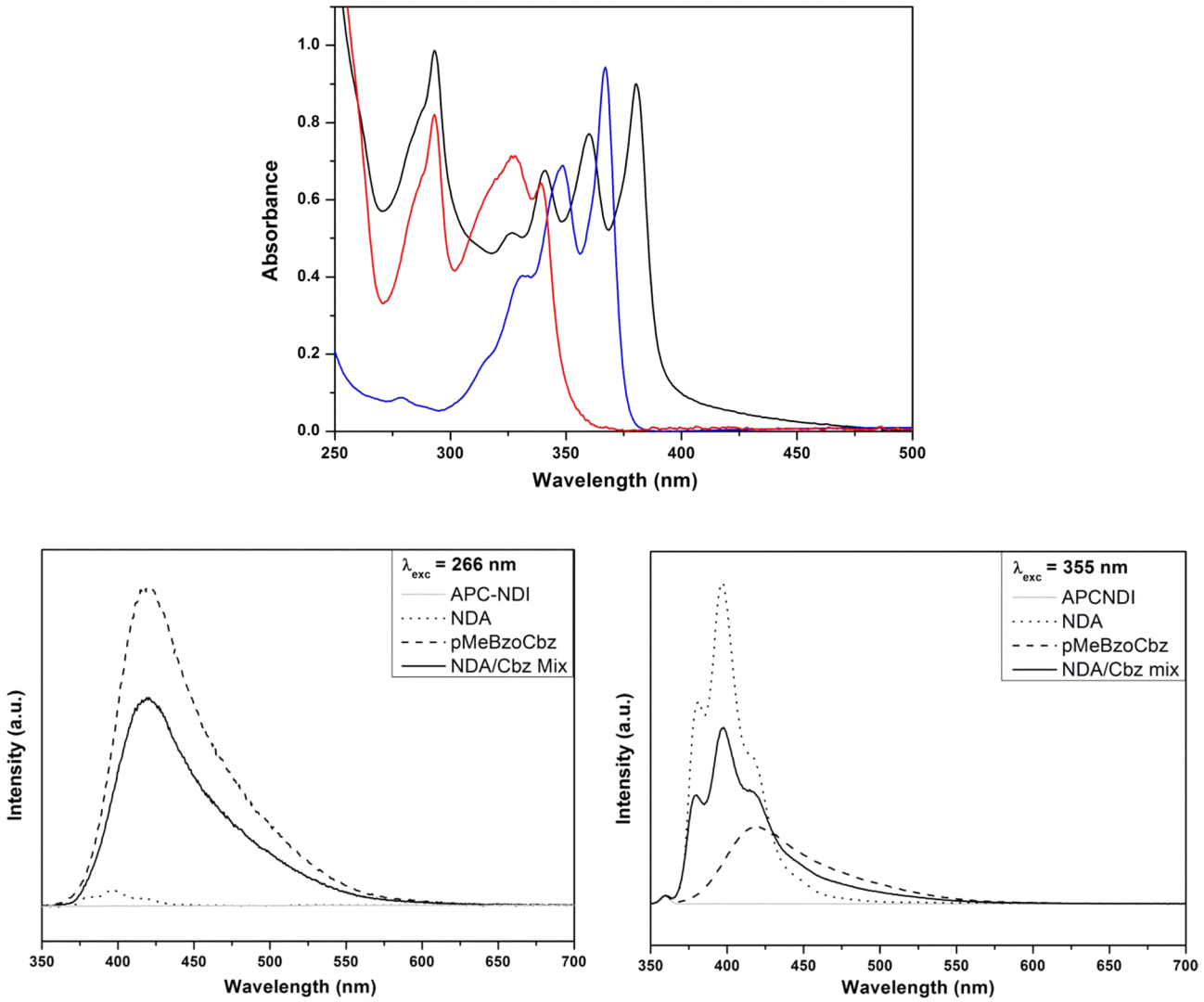

Figure 9. (Top) UV/vis absorption spectra of **APCNDI** (black), (*p*-carbazole)methyl benzoate (dotted line) and 1,4,5,8-naphthalenetetracarboxylic dianhydride (dashed line) and (bottom) emission spectra of equimolar solutions of 1,4,5,8-naphthalenetetracarboxylic dianhydride (**NDA**), (*p*-carbazole)methyl benzoate aminophenylcarbazole (*p*-CMbz), a 50/50 mixture of the **NDA** and *p*-**CMBz**, and **APCNDI**. Excitation at (left) 266 nm excites the carbazole unit selectively, while (right) at 355 nm both the p-**CMBz** and **NDA** components are excited.

Scheme 3. Photo-Induced Electron Transfer from a Carbazole (Cbz) Donor to a Naphthalene Diimide (NDI) Acceptor

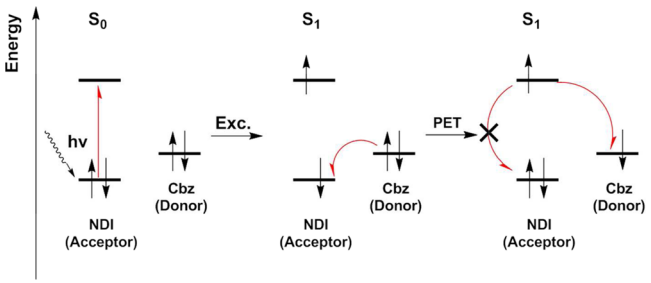

diimide and carbazole moieties of **APCNDI** is observed at λ_{exc} 355 nm (Figure 10). The bands at 1724 and 1685 cm^{-1} are assigned to naphthalene C═O stretching, while the carbazole C═C stretch is observed at 1627 cm^{-1} together with bands at 1608 and 1415 cm^{-1} assigned as naphthalene aromatic C═C and C−C stretching modes. Bands at 1111, 1073, and 1033 cm^{-1} are assigned to in-plane, and 713, 657, and 605 cm^{-1} to out-of-plane C−H bending modes of **APCNDI**. The bands at 1569, 1386, 858, 823, and 537 cm^{-1} are useful in assignment of the resonance Raman spectra of the polymer films formed (vide infra).

Cyclic Voltammetry of APCNDI. The redox chemistry of **APCNDI** between 0.0 and −1.7 V vs SCE is typical of an NDI (naphthalene) moiety with two reversible redox processes at −0.80 V and −1.20 V, with no evidence of polymer film formation even with repeated cycling between 0.0 and −1.7 V (Figure 11). The redox chemistry between 0.0 and 1.4 V vs SCE is identical to that of **APCCDI**, with efficient formation of a redox polymer film, as expected with sequential coupling of each carbazole moiety to build up a film of poly-**APCNDI** on the electrode. At a scan rate of 0.1 V s^{-1}, the cyclic voltammograms can undergo 100 segments while showing a steady increase of the redox response throughout. Although film thicknesses cannot be determined precisely from the redox response, due to incomplete charge transfer due to charge

DOI: 10.1021/acs.jpcc.7b04288
J. Phys. Chem. C 2017, 121, 14688−14702

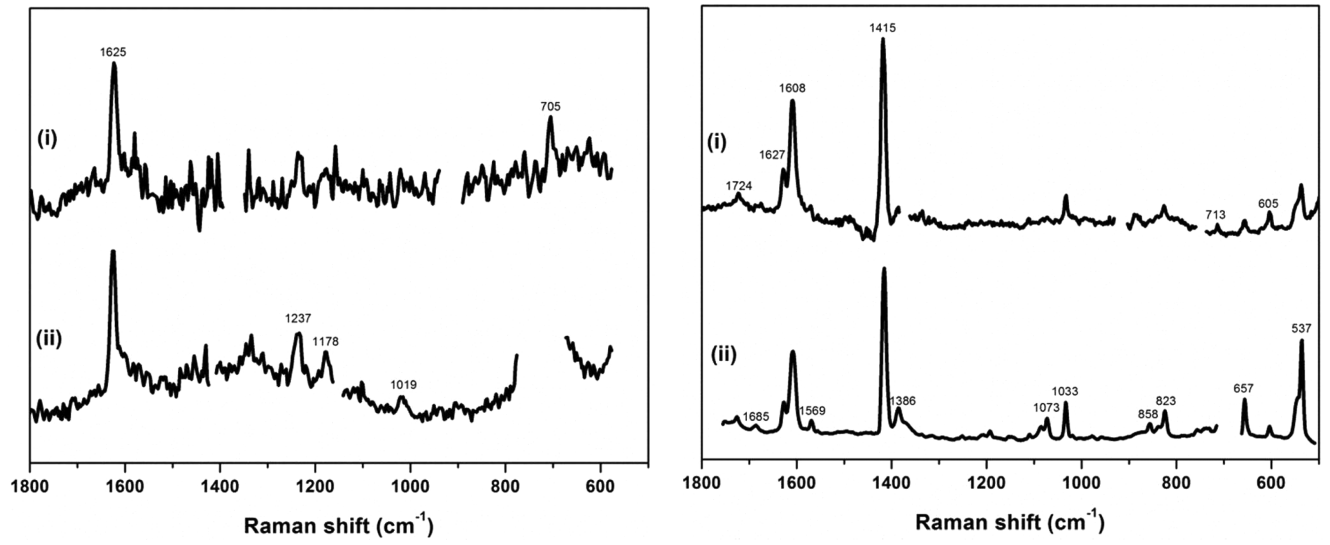

Figure 10. Resonance Raman spectra (λ_{exc} (left) 266 nm and (right) 355 nm) of **APCNDI** (i) in acetonitrile and (ii) in dichloromethane. *Distortions due to imperfect subtraction of Raman scattering of the solvent.

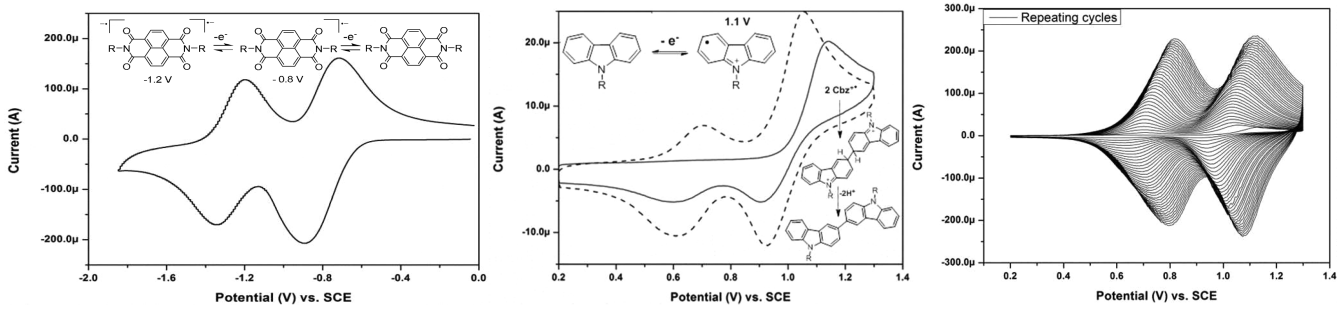

Figure 11. (Left) Reductive cyclic voltammetry of poly-**APCNDI** and (center) initial oxidative cyclic voltammetry of **APCNDI** (0.1 mM) in dichloromethane (0.1 V s^{-1}, 0.1 M $TBAPF_6$, argon purged, GC working electrode, with *iR* compensation applied) with assignment of redox processes. (Right) Repeated oxidative cyclic voltammetry of **APCNDI** showing a steady increase in signal for poly-**APCNDI**. SCE reference and platinum counter electrodes.

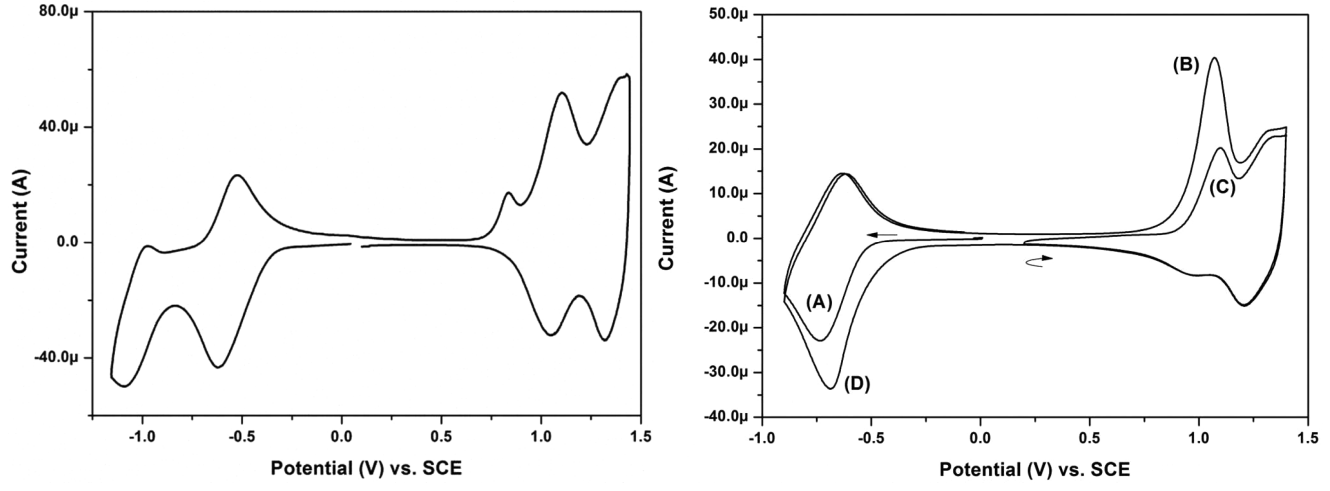

Figure 12. (left) Cyclic voltammetry of a poly-**APCNDI** modified platinum working electrode in monomer free dichloromethane (with 0.1 M $TBAPF_6$).The anodic wave at 0.8 V is due to release of trapped charges (vide infra) from reduction. Cathodic charge trapping, present in complete overlap with the reduction at −0.6 V here, is also observed clearly under monomer free conditions on an ITO working electrode (Figure S22). (Right) Cyclic voltammetry of a poly-**APCNDI** modified glassy carbon electrode in monomer free dichloromethane. Initial scan toward negative potentials from 0.0 V shows a reversible one electron redox wave (A) with a corresponding discharge peak (B) on the return cycle toward positive potentials which is absent on the second cycle in which the switching potential is 0.3 V. The third consecutive cycle to positive and the negative potentials shows a discharge peak due to trapped positive charges (D) (with 0.1 M $TBAPF_6$, platinum counter, and SCE reference electrode, scan rate 0.1 V s^{-1}). SCE reference and platinum counter electrodes.

DOI: 10.1021/acs.jpcc.7b04288
J. Phys. Chem. C 2017, 121, 14688−14702

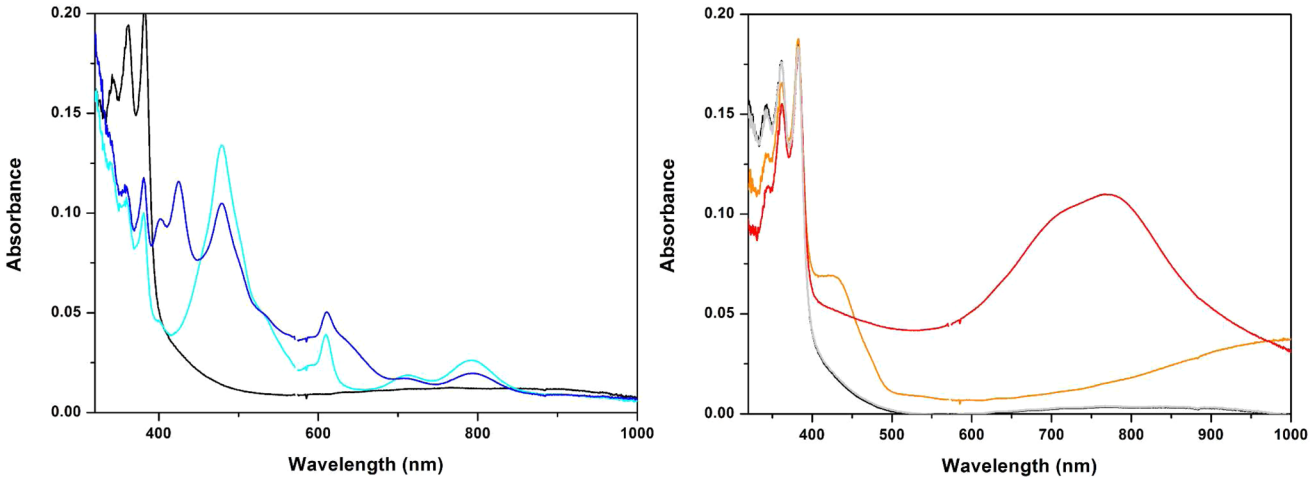

Figure 13. In situ UV/vis absorption spectroelectrochemistry of poly-**APCNDI** on an ITO slide (left) at 0.20 V (black), −0.90 V (light blue) and at −1.40 V (dark blue) and (right) at 0.00 V (black), 1.00 V (orange), 1.50 V (red), and at 0.00 V again (gray) in dichloromethane (0.1 M $TBAF_6$).

trapping (vide infra), an estimation can be made of the upper and lower limits of surface coverage by comparing cathodic and anodic charge passed. The surface coverages determined under these conditions are between 1.2 and 1.6 * 10^{-9} mol cm^{-2} at a glassy carbon electrode, which when compared with typical monolayer coverages that are the range of 10^{-10} to 10^{-11} mol cm^{-2}, indicates ca. 10 to 15 monolayer equivalents.[69] Discharge peaks are observed during cyclic voltammetry, in monomer containing solution, typically after the third or fourth cycle and grow incrementally thereafter. Surface coverage at this point is estimated to be between 1.5 and 1.8 × 10^{-10} mol cm^{-2}, which is in the order of a one to two monolayers.

The redox response of the poly-**APCNDI** formed on a range of electrode types is retained upon washing and transferring to monomer free solution (Figure 12) and are stable under repeated cycling between 0.2 and 1.2 V, confirming the chemical and mechanical robustness of the films, i.e., with regard to adventitious water and oxygen. Notably, when performing cyclic voltammetry over the potential range of both redox-active species, i.e., between −1.0 and 1.4 V, a prepeak to either or both of the cathodic and anodic processes appears (Figure 12). This occurrence was assigned to charge trapping, the characterization of which will be discussed below. A linear dependence of current of the main redox waves on scan rate (up to 2 V s^{-1}) is observed as expected for a surface confined redox process (Figure S21).

UV/vis−NIR Absorption Spectroelectrochemistry of poly-APCNDI. The UV/vis absorption spectrum of poly-**APCNDI** resembles that of the monomer with the characteristic vibronic structure of the naphthalene diimide unit red-shifted slightly (Figure S23). UV/vis absorption spectra of poly-**APCNDI** on an ITO on glass electrode in several oxidation states are shown in Figure 13. Reduction results in the appearance of a characteristic absorption band at 480 nm corresponding to the NDI monoanion (at −0.90 V), concomitant with a decrease in the absorption of the NDI unit at 390 nm. At more negative potentials, a band at 425 nm appears corresponding to the NDI dianion (at −1.40 V), concomitant with a decrease in the absorbance of the NDI monoanion at 480 nm (Figure 13). Complete conversion to the NDI dianion, i.e., a complete loss in absorbance of the NDI monoanion at 710 and 790 nm, was not achieved, indicating that Coulombic interactions are not fully compensated by uptake of cations (TBA^+) from the electrolyte. Scaled subtraction of the UV/vis absorption spectrum of the NDI monoanion reveals the absorption spectrum of the NDI dianion (Figure S24). Notably, subsequent oxidation at 0.0 V does not lead to a full recovery of the original absorption spectrum with residual absorbance of the NDI monoanion consistent with kinetic charge trapping in the film (Figure S25, vide infra). UV/vis spectra recorded during cyclic voltammetry between 0.00 to 1.60 V showed the appearance of NIR absorptions assigned to the monocationic (425 and 1200 nm, at 1.00 V, Figure S26) and dicationic (775 nm, at 1.5 V) states of the bis-carbazole units (Figure 13) and a decrease in bis-carbazole absorption at 325 nm. The absorbance of the NDI unit is unaffected by oxidation. The combination of NDI and **APC** units allow for access to five distinct redox states and control of absorption over the entire UV/vis−NIR spectral range, and in particular the visible region which is not accessed easily with polymers comprising of carbazole units alone.[70]

Resonance Raman Spectroelectrochemistry of poly-APCNDI. In situ Raman spectroscopy, at λ_{exc} 785 nm allowed for characterization of the **APCNDI** monocation, dication, and monoanion states, making use of resonance enhancement due to the absorption of these states at this wavelength (Figure 14, vide infra). Continuous monitoring by Raman spectroscopy during cyclic voltammetry on a polymer modified platinum electrode between 0.20 and 1.30 V shows the appearance of weak bands at 1622, 1592, and 702 cm^{-1} upon oxidation between 0.7 and 1.0 V. At potentials above 1.1 V, additional bands were enhanced substantially also together with a change in the relative intensity of the bands at ca. 1600 cm^{-1}. These bands disappeared upon subsequent reduction. The increased intensity observed for the dication state compared with that for the monocation state is consistent with the increased absorbance at 785 nm for the former (Figure 13). The relative intensity of the bands of the weakly scattering monocationic species allows them to be distinguished easily from those of the dicationic species and are in both cases assigned to the bis-carbazole unit.

The resonance enhanced Raman bands (at λ_{exc} 266 nm) of **APCNDI** at 1622 and 705 cm^{-1} (Figure 10) are assigned to C═C stretching and C−H out of plane bending of the carbazole moieties and correspond with bands observed for the mono- and dication states of poly-**APCNDI**. The bands at 1172

DOI: 10.1021/acs.jpcc.7b04288
J. Phys. Chem. C 2017, 121, 14688−14702

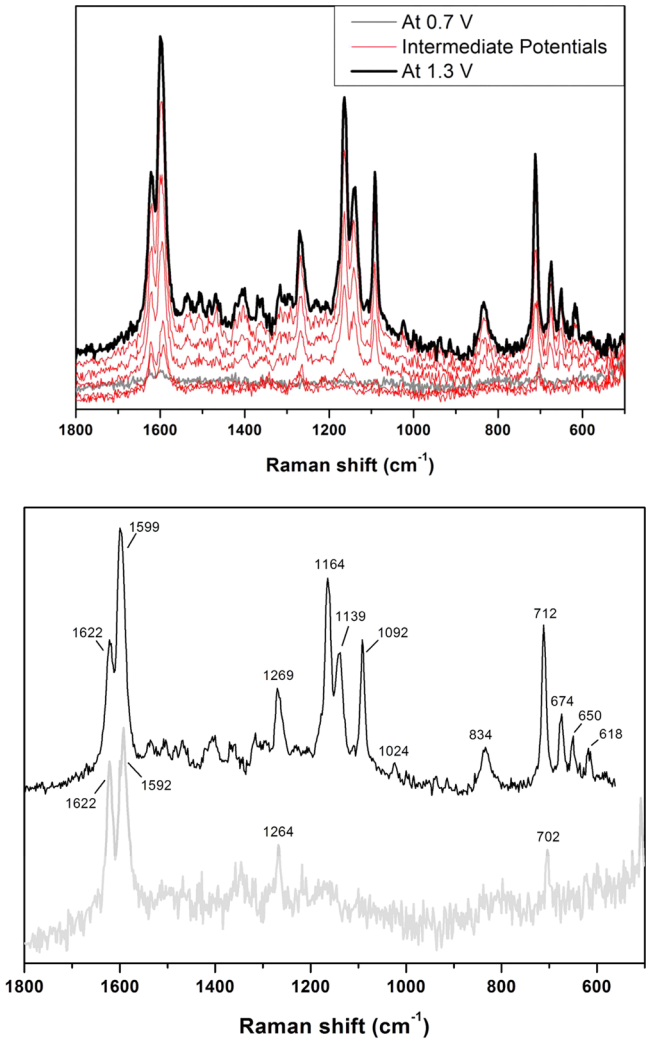

Figure 14. (Upper) In situ Raman spectroelectrochemistry of poly-**APCNDI** at a Pt working electrode, scanning the potential from 0.7 to 1.3 V at 5 mV s^{-1} (in dichloromethane with 0.1 M $TBAPF_6$, λ_{exc} 785 nm) and (lower) comparison of the dication species formed at 1.3 V (i) and the monocation species at 1.0 V (ii).

and 1020 cm^{-1} correspond to bands observed here at 1164 and 1024 cm^{-1}, assigned to in plane bending of the oxidized carbazole C−H modes. Additionally, the appearance of a band at 1269 cm^{-1} was assigned as a C−N stretching mode, which is close to the band observed at 1237 cm^{-1} in the spectrum of the monomer (at λ_{exc} 266 nm), the shift to higher wavenumber being consistent with the increased bond strenght expected in the cationic state (i.e., increased C═N character). The carbazole C═C stretching band at 1622 cm^{-1} is unchanged upon oxidation, while the stronger band shifts from 1594 to 1599 cm^{-1} (also observed in the ex situ Raman measurements, vide infra) and gains intensity relatively to the 1622 cm^{-1} band. Furthermore, a shoulder at 1653 cm^{-1} is observed in the monocationic state, assigned to the C═C alkene stretch due to loss of aromaticity through the radical character of the monocation. The band at 704 cm^{-1} observed for the monomer at λ_{exc} 266 nm, assigned to a C−H out of plane bending mode of **APCNDI**, shifts to 712 cm^{-1} upon further oxidation to the dicationic state. In the case of the dicationic state, the bands at 1164, 1140, and 1092 cm^{-1} are assigned as in plane, and 675, 651, and 618 cm^{-1} as out of plane C−H bending modes, constituting shifts of up to 30 cm^{-1} from those modes observed in resonance Raman spectrum of the monomer.

Charge Trapping in poly-APCNDI Films. In contrast to **APCCDI**, for **APCNDI** a prepeak to both oxidation and reduction waves was observed on a range of electrodes (including glassy carbon, platinum, and gold macroelectrodes and ITO coated glass slides), indicative of charge trapping.[71] For example, at a gold macroelectrode, additional redox waves were observed at 0.80 V and at −0.50 V during formation of poly-**APCNDI** in the cyclic voltammetry of **APCNDI** (Figure 15). Charge trapping was first reported by Murray et al. in 1981[35] and is due to the confinement of charges in the polymer film through defects (i.e., thermodynamic—where a distinct species with a redox potential less positive or less negative than the polymer is formed) or where the outer layer is unable to discharge before the inner layer is depolarized (i.e., kinetic—where polymer film is sufficiently thick that the inner layer insulates the outer layer from the potential gradient at the electrode, Figure 15).

The increase in the discharge peak current and shift to more positive/negative potential with cycle number and hence film thickness are apparent during the polymerization of **APCNDI** by cyclic voltammetry (Figure 15). These shifts reflect an increase in the distance between the outer edge of the polymer film and the limit to the thickness of film at the electrode that can be discharged directly. This, however, does not imply that charge trapping does not occur in films of poly-**APCCDI** (vide supra), albeit that the trapped positive charges are not released by film reduction due to the absence of an accessible reduction wave. The formation and release of trapped charges can be observed by cyclic voltammetry, UV/vis absorption (Figure 13), and resonance Raman spectroscopy providing dual redox-functionality of electrochromism and nonvolatile 3-state memory (reduced, neutral, oxidized)

Raman spectra recorded at a poly-**APCNDI** modified Au electrode enables identification of the species responsible for the charge trapping, with spectra recorded, ex-situ, of charged films showing Raman bands that confirm that the species responsible for charge trapping are in both cases the one electron oxidized and reduced states (Figure 16).

C═C stretching modes at 1620 and 1594 cm^{-1} are observed, which correspond to a one electron oxidized bis-carbazole species. The spectrum of the positively charge trapped film shows a shoulder at 1620 cm^{-1} and a shift toward 1594 cm^{-1} by the scattering maximum at 1598 cm^{-1}. Additionally, Raman bands at 1341, 1267, 718, and 588 cm^{-1} appear both upon oxidation and in the film that had undergone a cycle to positive potentials and subsequently to 0.0 V. Upon both reduction of the polymer film and after a reductive cycle in which the potential is returned to 0.0 V, bands at 1413 and 1374 cm^{-1} are observed. Furthermore, these bands decrease in intensity concomitantly with the appearance bis-carbazole monocation modes upon oxidation. The band at 1413 cm^{-1} is assigned to a naphthalene aromatic C−C stretching by comparison with the resonance Raman spectrum of **APCNDI** monomer recorded at λ_{exc} 355 nm. Similarly, the bands at 541 and 1374 cm^{-1} correspond to those at 537 and 1386 cm^{-1}, respectively, in **APCNDI**. Hence, positive or negative charges trapped in the polymer film can be assigned as due to kinetically trapped cationic and anionic forms of the bis-carbazole and NDI moieties, respectively.

Erasing and rewriting this three state charge trapping system can be achieved by application of positive and negative

DOI: 10.1021/acs.jpcc.7b04288
J. Phys. Chem. C 2017, 121, 14688−14702

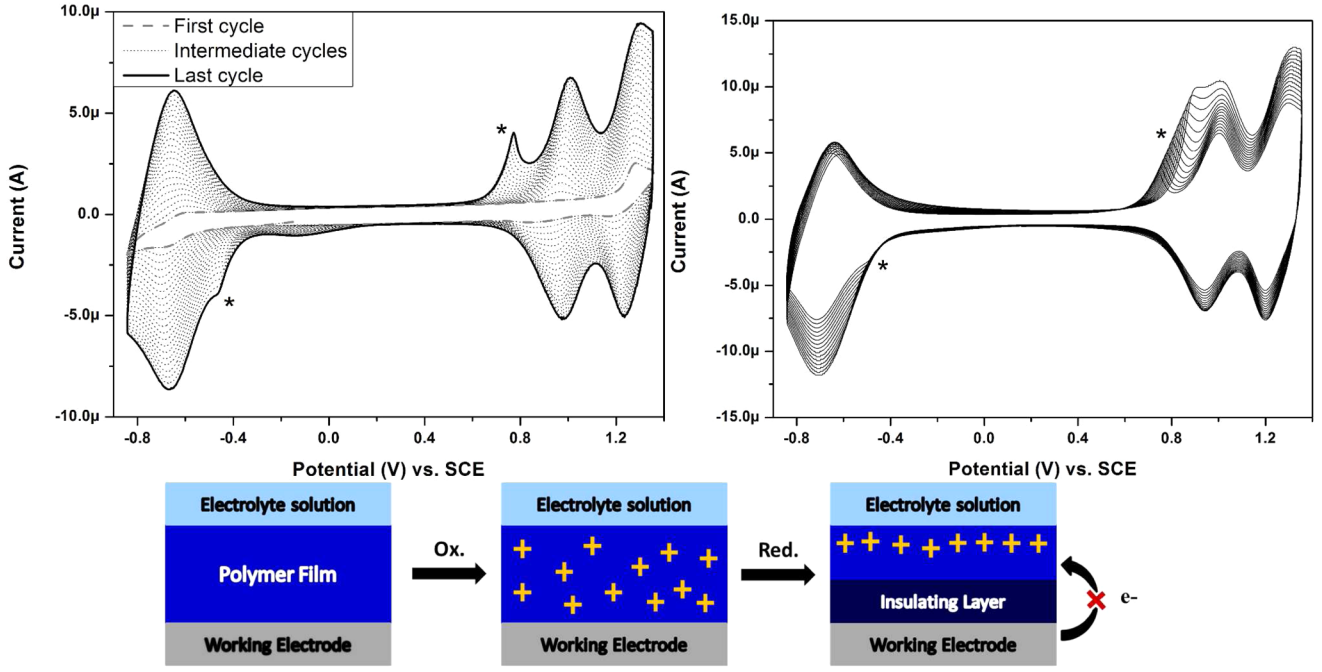

Figure 15. poly-**APCNDI** film formation via repetitive cyclic voltammetry at a gold macroelectrode (0.067 mM in dichloromethane with 0.1 M $TBAPF_6$, scan rate 0.1 V s^{-1}, inert atmosphere, with Ag/AgCl reference and Pt counter electrode). Left: initial cycle(s) and right: later cycles. The prepeaks "*" are due to discharge of kinetically trapped charges.

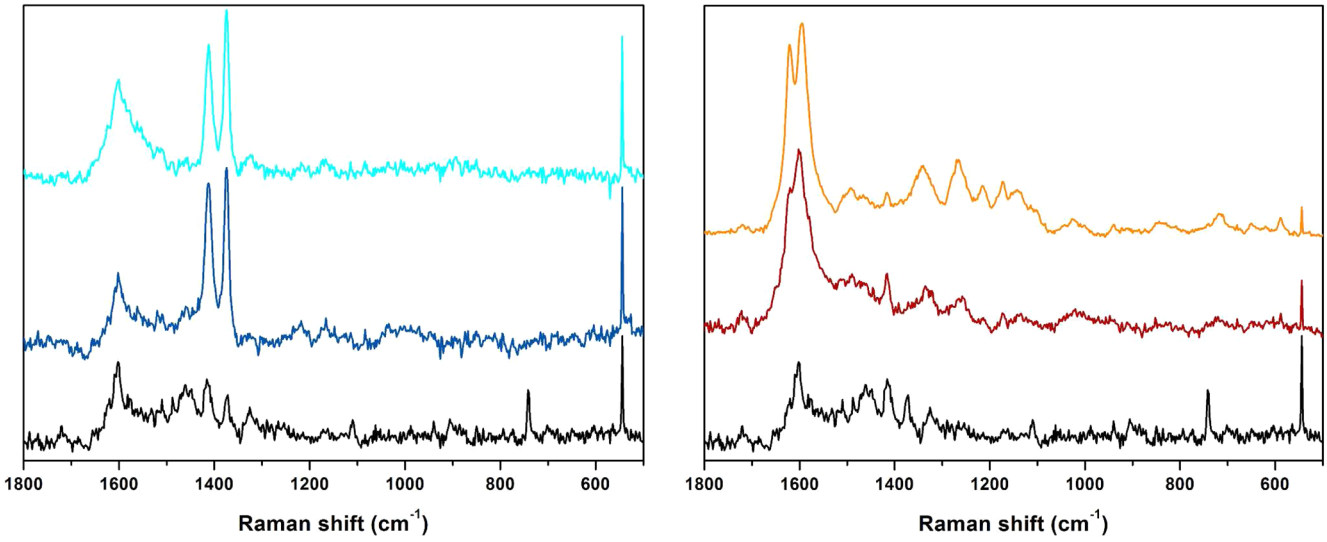

Figure 16. Ex situ Raman spectroscopy (λ_{exc} 785 nm) of a poly-**APCNDI** modified Au working electrode. Recorded states include the discharged (by cycling to −0.5 and 0.8 V in order to release negatively (left) and positively (right) trapped charges, respectively, solid black lines), charge trapped (by cycling to −0.9 V (left) or 1.1 V (right) and back, blue, and red lines), and fully charged state (by pausing the cyclic voltammogram at either −0.9 (left) or 1.1 (right) V, cyan and orange lines). In dichloromethane with 0.1 M $TBAPF_6$ at a scan rate of 0.5 V s^{-1}.

potentials (Figure 17). Reduction of the film followed by polarization of the electron to 0.0 V resulted in the appearance of a discharge peak on cycling to positive potentials even after a 30 min delay.

CONCLUSIONS

The design of multifunctional surfaces and especially redox functional surfaces based on molecular components necessitates the proper orthogonal functioning of not only the "active" components but also the components required for polymer film formation. In this contribution, we show that oxidative C−C coupling of carbazole is a versatile approach to the formation of stable redox polymer films when two carbazole units are tethered appropriately so as to enable sequential dimerization and thereby stepwise polymer growth. The key advantage to the bis-carbazole unit in polymer film formation is that the redox potential for the oxidation of monomer is coincident with that of the second oxidation of the bis-carbazole unit, thereby avoiding film growth limitations seen with earlier systems. The unit connecting the two carbazole units is key to achieving this and in the present study an amino phenyl unit helps to lower the redox potential of the carbazole unit, however, the use of a diimide group in the bridge is

DOI: 10.1021/acs.jpcc.7b04288
J. Phys. Chem. C 2017, 121, 14688−14702

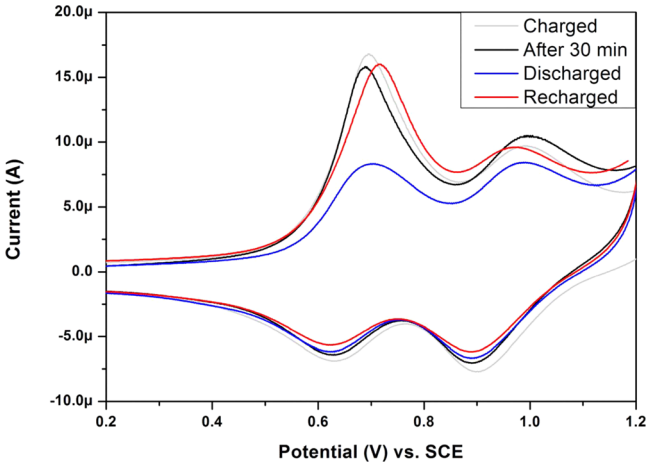

Figure 17. Sequential cyclic voltammetry of a gold macro electrode poly-**APCNDI** modified film in monomer free solution (dichloromethane with 0.1 M $TBAPF_6$, scan rate 0.1 V s^{-1}, with Ag/AgCl reference and Pt counter electrode, "n-charging" carried out by a reductive cycle to −0.9 V). Cyclic voltammograms were recorded of a charged film, read-out after 30 min storage in air while charged, a subsequently discharged film, and thereafter immediately recharged film. Similar data showing charge storage over 6 days is shown in Figure S27.

essential to preclude interference by the formally, *p*-diaminobenzene motif. The various precursors led to the design of the multifunctional electro-polymerizable unit through insertion of an additional redox active naphthalene group to form **APCNDI**. Interestingly, whereas poly-**APCCDI** shows redox switchable photoluminescence, the **APCNDI** Donor−Acceptor−Donor system exhibits complete quenching of emission through intramolecular photoinduced electron transfer between the **NDI** and **APC** moieties. The quenching is sufficient to enable characterization of poly-**APCNDI** films in several redox states by resonance Raman spectroscopy. In particular, we demonstrate that charge trapping in sufficiently thick films of poly-**APCNDI** is kinetic and not thermodynamic.

Although resonance Raman microspectroscopy is used in the present study primarily to characterize the species responsible for charge trapping as kinetic and not thermodynamic, read can be achieved by UV/vis absorption spectroscopy and electrochemically. However, although a possible advantage of Raman microspectroscopy is found in the specificity of the molecular information contained within the spectra and high spatial resolution, ultimately charge trapping is useful in electrical readout systems despite the destructive nature of such readout. In summary, the combination of facile polymer film formation with highly controllable film thickness together with retention of the properties of the monomer **APCNDI** in the films, provide for a 3-state nonvolatile memory with nondestructive optical readout and by resonance Raman spectroscopy.

■ ASSOCIATED CONTENT

Supporting Information

The Supporting Information is available free of charge on the ACS Publications website at DOI: 10.1021/acs.jpcc.7b04288.

Details of synthesis and characterization, additional FTIR, Raman, ^{1}H NMR, and UV/vis absorption spectral and electrochemical data (PDF)

■ AUTHOR INFORMATION

Corresponding Author

*E-mail: w.r.browne@rug.nl (W.R.B.).

ORCID

Wesley R. Browne: 0000-0001-5063-6961

Notes

The authors declare no competing financial interest.

■ ACKNOWLEDGMENTS

Financial support comes from the Ministry of Education, Culture and Science (Gravity program 024.001.035, L.K., W.R.B.).

■ REFERENCES

(1) Russell, T. P. Surface-Responsive Materials. *Science* **2002**, *297*, 964−967.
(2) Yerushalmi, R.; Scherz, A.; van der Boom, M. E.; Kraatz, H.-B. Stimuli Responsive Materials: New Avenues toward Smart Organic Devices. *J. Mater. Chem.* **2005**, *15*, 4480−4487.
(3) Katsonis, N.; Lubomska, M.; Pollard, M. M.; Feringa, B. L.; Rudolf, P. Synthetic Light-Activated Molecular Switches and Motors on Surfaces. *Prog. Surf. Sci.* **2007**, *82*, 407−434.
(4) Raymo, F. M.; Giordani, S.; White, A. J. P.; Williams, D. J. *J.* Digital Processing with a Three-State Molecular Switch. *J. Org. Chem.* **2003**, *68*, 4158−4169.
(5) Flood, A. H.; Stoddart, J. F.; Steuerman, D. W.; Heath, J. R. CHEMISTRY: Enhanced: Whence Molecular Electronics? *Science* **2004**, *306*, 2055−2056.
(6) Deb, S. K. A Novel Electrophotographic System. *Appl. Opt.* **1969**, *8*, 192−195.
(7) Ling, Q.; Liaw, D.; Zhu, C.; Chan, D.; Kang, E.; Neoh, K. Polymer Electronic Memories: Materials, Devices and Mechanisms. *Prog. Polym. Sci.* **2008**, *33*, 917−978.
(8) Heremans, P.; Gelinck, G. H.; Muller, R.; Baeg, K. J.; Kim, D. Y.; Noh, Y. Y. Polymer and Organic Nonvolatile Memory Devices. *Chem. Mater.* **2011**, *23*, 341−358.
(9) Liu, Y.-L.; Wang, K.-L.; Huang, G.-S.; Zhu, C.-X.; Tok, E.-S.; Neoh, K.-G.; Kang, E.-T. Volatile Electrical Switching and Static Random Access Memory Effect in a Functional Polyimide Containing Oxadiazole Moieties. *Chem. Mater.* **2009**, *21*, 3391−3399.
(10) Liu, Y.-L.; Ling, Q.-D.; Kang, E.-T.; Neoh, K.-G.; Liaw, D.-J.; Wang, K.-L.; Liou, W.-T.; Zhu, C.-X.; Chan, D. S.-H. Volatile Electrical Switching in a Functional Polyimide Containing Electron-Donor and Acceptor Moieties. *J. Appl. Phys.* **2009**, *105*, 044501.
(11) Wang, K. L.; Liu, Y. L.; Shih, I. H.; Neoh, K. G.; Kang, E. T. Synthesis of Polyimides Containing Triphenylamine-Substituted Triazole Moieties for Polymer Memory Applications. *J. Polym. Sci., Part A: Polym. Chem.* **2010**, *48*, 5790−5800.
(12) Ling, Q. D.; Chang, F. C.; Song, Y.; Zhu, C. X.; Liaw, D. J.; Chan, D. S. H.; Kang, E. T.; Neoh, K. G. Synthesis and Dynamic Random Access Memory Behavior of a Functional Polyimide. *J. Am. Chem. Soc.* **2006**, *128*, 8732−8733.
(13) Wang, K. L.; Liu, Y. L.; Lee, J. W.; Neoh, K. G.; Kang, E. T. Nonvolatile Electrical Switching and Write-Once Read-Many-Times Memory Effects in Functional Polyimides Containing Triphenylamine and 1,3,4-Oxadiazole Moieties. *Macromolecules* **2010**, *43*, 7159−7164.
(14) Lee, W.-Y.; Kurosawa, T.; Lin, S.-T.; Higashihara, T.; Ueda, M.; Chen, W.-C. New Donor−Acceptor Oligoimides for High-Performance Nonvolatile Memory Devices. *Chem. Mater.* **2011**, *23*, 4487−4497.
(15) Liu, C. L.; Chen, W. C. Donor−Acceptor Polymers for Advanced Memory Device Applications. *Polym. Chem.* **2011**, *2*, 2169−2174.
(16) Zhang, E.; Wang, W.; Zhang, C.; Jin, Y.; Zhu, G.; Sun, Q.; Zhang, D. W.; Zhou, P.; Xiu, F. Tunable Charge-Trap Memory Based on Few-Layer MoS_2. *ACS Nano* **2015**, *9*, 612−619.

DOI: 10.1021/acs.jpcc.7b04288
J. Phys. Chem. C 2017, 121, 14688−14702

(17) Zhao, Z.; Xing, Y.; Wang, Z.; Lu, P. Dual-Fluorescent Donor−Acceptor Dyad with Tercarbazole Donor and Switchable Imide Acceptor: Promising Structure for an Integrated Logic Gate. *Org. Lett.* **2007**, *9*, 547−550.
(18) Sartin, M. M.; Huang, C.; Marshall, A. S.; Makarov, N.; Barlow, S.; Marder, S. R.; Perry, J. W. Nonlinear Optical Pulse Suppression via Ultrafast Photoinduced Electron Transfer in an Aggregated Perylene Diimide/Oligothiophene Molecular Triad. *J. Phys. Chem. A* **2014**, *118*, 110−121.
(19) Huang, C.; Sartin, M. M.; Cozzuol, M.; Siegel, N.; Barlow, S.; Perry, J. W.; Marder, S. R. Photoinduced Electron Transfer and Nonlinear Absorption in Poly(carbazole-alt-2,7-fluorene)s Bearing Perylene Diimides as Pendant Acceptors. *J. Phys. Chem. A* **2012**, *116*, 4305−4317.
(20) Milder, M. T. W.; Herek, J. L.; Areephong, J.; Feringa, B. L.; Browne, W. R. Tunable Aggregation and Luminescence of Bis-Diarylethene-Sexithiophenes. *J. Phys. Chem. A* **2009**, *113*, 7717−7724.
(21) Kortekaas, L.; Browne, W. R. Solvation Dependent Redox-Gated Fluorescence Emission in a Diarylethene-Based Sexithiophene Polymer Film. *Adv. Opt. Mater.* **2016**, *4*, 1378−1384.
(22) Grazulevicius, J. V.; Strohriegl, P.; Pielichowski, J.; Pielichowski, K. Carbazole-Containing Polymers: Synthesis, Properties and Applications. *Prog. Polym. Sci.* **2003**, *28*, 1297−1353.
(23) Thomas, K. R. J.; Lin, J. T.; Tao, Y.-T.; Ko, C.-W. Light-Emitting Carbazole Derivatives: Potential Electroluminescent Materials. *J. Am. Chem. Soc.* **2001**, *123*, 9404−9411.
(24) Wu, Y.; Li, Y.; Gardner, S.; Ong, B. S. Indolo[3,2-b]carbazole-Based Thin-Film Transistors with High Mobility and Stability. *J. Am. Chem. Soc.* **2005**, *127*, 614−618.
(25) Kang, E. S. H.; Yuen, J. D.; Walker, W.; Coates, N. E.; Cho, S.; Kim, E.; Wudl, F. Amorphous Dithenylcyclopentadienone-Carbazole Copolymer for Organic Thin-Film Transistors. *J. Mater. Chem.* **2010**, *20*, 2759−2765.
(26) Li, J.; Grimsdale, A. C. Carbazole-Based Polymers for Organic Photovoltaic Devices. *Chem. Soc. Rev.* **2010**, *39*, 2399−2410.
(27) Tomkeviciene, A.; Grazulevicius, J. V.; Kazlauskas, K.; Gruodis, A.; Jursenas, S.; Ke, T.; Wu, C.-C. Impact of Linking Topology on the Properties of Carbazole Trimers and Dimers. *J. Phys. Chem. C* **2011**, *115*, 4887−4897.
(28) Xu, B.; Sheibani, E.; Liu, P.; Zhang, J.; Tian, H.; Vlachopoulos, N.; Boschloo, G.; Kloo, L.; Hagfeldt, A.; Sun, L. Carbazole-Based Hole-Transport Materials for Efficient Solid-State Dye-Sensitized Solar Cells and Perovskite Solar Cells. *Adv. Mater.* **2014**, *26*, 6629−6634.
(29) Xu, Q.-C.; Wang, X.-F.; Xing, G.-W.; Zhang, Y. Substituted 2-Aminobenzamide Compounds: Synthesis, Fluorescence ON−OFF−ON Sensing of Zn(II) and PPi Ions, Assay for Alkaline Phosphatase, and Computational Study. *RSC Adv.* **2013**, *3*, 15834−15841.
(30) Kricheldorf, H. R. Photoconducting Polymers. *Handbook of Polymer Synthesis: Part B (in Two Parts); Plastics Engineering*; CRC Press: New York, 1991; pp 1410−1422.
(31) Natori, I. Anionic Polymerization of N-Vinylcarbazole with Alkyllithium as an Initiator. *Macromolecules* **2006**, *39*, 6017−6024.
(32) Koyuncu, F. B. An Ambipolar Electrochromic Polymer Based on Carbazole and Naphthalene Bisimide: Synthesis and Electro-Optical Properties. *Electrochim. Acta* **2012**, *68*, 184−191.
(33) Karon, K.; Lapkowski, M. Carbazole electrochemistry: a short review. *J. Solid State Electrochem.* **2015**, *19*, 2601−2610.
(34) Cloutet, E.; Olivero, C.; Adès, D.; Castex, M.-C.; Siove, A. Synthesis and Blue Luminescence of a Soluble Newly Designed Carbazole Main-Chain Polymer. *Polymer* **2002**, *43*, 3489−3495.
(35) Ivashenko, O.; van Herpt, J. T.; Rudolf, P.; Feringa, B. L.; Browne, W. R. Oxidative Electrochemical Aryl C-C Coupling of Spiropyrans. *Chem. Commun.* **2013**, *49*, 6737−9.
(36) Mizoguchi, T.; Adams, R. N. Anodic Oxidation Studies of N,N-Dimethylaniline. I. Voltammetric and Spectroscopic Investigations at Platinum Electrodes. *J. Am. Chem. Soc.* **1962**, *84*, 2058−2061.
(37) Galus, Z.; White, R. M.; Rowland, F. S.; Adams, R. N. Anodic Oxidation Studies of N,N-Dimethylaniline. III. Tritium Tracer Studies of Electrolysis Products. *J. Am. Chem. Soc.* **1962**, *84*, 2065−2068.
(38) Yang, H.; Wipf, D. O.; Bard, A. J. Application of Rapid Scan Cyclic Voltammetry to a Study of the Oxidation and Dimerization of N,N-Dimethylaniline in Acetonitrile. *J. Electroanal. Chem.* **1992**, *331*, 913−924.
(39) Kortekaas, L.; Ivashenko, O.; van Herpt, J. T.; Browne, W. R. A Remarkable Multitasking Double Spiropyran: Bidirectional Visible-Light Switching of Polymer-Coated Surfaces with Dual Redox and Proton Gating. *J. Am. Chem. Soc.* **2016**, *138*, 1301−1312.
(40) Koyuncu, S.; Zafer, C.; Koyuncu, F. B.; Aydin, B.; Can, M.; Sefer, E.; Ozdemir, E.; Icli, S. A New Donor−Acceptor Double-Cable Carbazole Polymer with Perylene Bisimide Pendant Group: Synthesis, Electrochemical, and Photovoltaic Properties. *J. Polym. Sci., Part A: Polym. Chem.* **2009**, *47*, 6280−6291.
(41) Koyuncu, F. B.; Koyuncu, S.; Ozdemir, E. A Novel Donor−Acceptor Polymeric Electrochromic Material Containing Carbazole and 1,8-Naphtalimide as Subunit. *Electrochim. Acta* **2010**, *55*, 4935−4941.
(42) Logtenberg, H.; Jellema, L-J. C.; Lopez-Martinez, M. J.; Areephong, J.; Verpoorte, E.; Feringa, B. L.; Browne, W. R. In Situ Monitoring of Polymer Redox States by Resonance μRaman Spectroscopy and Its Applications in Polymer Modified Microfluidic Channels. *Anal. Methods* **2012**, *4*, 73−79.
(43) Wesenhagen, P.; Areephong, J.; Fernandez Landaluce, T.; Heureux, N.; Katsonis, N.; Hjelm, J.; Rudolf, P.; Browne, W. R.; Feringa, B. L. Photochromism and Electrochemistry of a Dithienylcyclopentene Electroactive Polymer. *Langmuir* **2008**, *24*, 6334−6342.
(44) Areephong, J.; Kudernac, T.; de Jong, J. J. D.; Carroll, G. T.; Pantorott, D.; Hjelm, J.; Browne, W. R.; Feringa, B. L. On/Off Photoswitching of the Electropolymerizability of Terthiophenes. *J. Am. Chem. Soc.* **2008**, *130*, 12850−12851.
(45) Ashton, P. R.; Boyd, S. E.; Brindle, A.; Langford, S. J.; Menzer, S.; Perez-Garcıa, L.; Preece, J. A.; Raymo, F. M.; Spencer, F. M.; Stoddart, J. F.; White, A. J. P.; Williams, D. J. Diazapyrenium-Containing Catenanes and Rotaxanes. *New J. Chem.* **1999**, *23*, 587−602.
(46) Iijima, T.; Vignon, S. A.; Tseng, H. R.; Jarrosson, T.; Sanders, J. K. M.; Marchioni, F.; Venturi, M.; Apostoli, E.; Balzani, V.; Stoddart, J. F. Controllable Donor-Acceptor Neutral [2]Rotaxanes. *Chem. - Eur. J.* **2004**, *10*, 6375−6392.
(47) Fallon, G. D.; Lee, M. A.-P.; Langford, S. J.; Nichols, P. J. Unusual Solid-State Behavior in a Neutral [2]Catenane Bearing a Hydrolyzable Component. *Org. Lett.* **2004**, *6*, 655−658.
(48) Hansen, J. G.; Feeder, N.; Hamilton, D. G.; Gunter, M. J.; Becher, J.; Sanders, J. K. M. Macrocyclisation and Molecular Interlocking via Mitsunobu Alkylation: Highlighting the Role of C−H···O Interactions in Templating. *Org. Lett.* **2000**, *2*, 449−452.
(49) Pantoş, G. D.; Pengo, P.; Sanders, J. K. M. Hydrogen-Bonded Helical Organic Nanotubes. *Angew. Chem., Int. Ed.* **2007**, *46*, 194−197.
(50) Talukdar, P.; Bollot, G.; Mareda, J.; Sakai, N.; Matile, S. Ligand-Gated Synthetic Ion Channels. *Chem. - Eur. J.* **2005**, *11*, 6525−6532.
(51) Lokey, R. S.; Iverson, B. L. Synthetic Molecules that Fold into a Pleated Secondary Structure in Solution. *Nature* **1995**, *375*, 303−305.
(52) Sakai, N. P.; Charbonnaz; Ward, S.; Matile, S. Ion-Gated Synthetic Photosystems. *J. Am. Chem. Soc.* **2014**, *136*, 5575−5578.
(53) Takenaka, S.; Yamashita, K.; Takagi, M.; Uto, Y.; Kondo, H. DNA Sensing on a DNA Probe-Modified Electrode Using Ferrocenylnaphthalene Diimide as the Electrochemically Active Ligand. *Anal. Chem.* **2000**, *72*, 1334−1341.
(54) Bhosale, S. V.; Jani, C. H.; Langford, S. Chemistry of Naphthalene Diimides. *Chem. Soc. Rev.* **2008**, *37*, 331−342.
(55) Dawson, R.; Hennig, E. A.; Weimann, D. P.; Emery, D.; Ravikumar, V.; Montenegro, J.; Takeuchi, T.; Gabutti, S.; Mayor, M.; Mareda, J.; Schalley, C. A.; Matile, S. Experimental Evidence for the Functional Relevance of Anion−π Interactions. *Nat. Chem.* **2010**, *2*, 533−538.
(56) Guha, S.; Goodson, F. S.; Roy, S.; Corson, L. J.; Gravenmier, C. A.; Saha, S. Electronically Regulated Thermally and Light-Gated Electron Transfer from Anions to Naphthalenediimides. *J. Am. Chem. Soc.* **2011**, *133*, 15256−15259.

DOI: 10.1021/acs.jpcc.7b04288
J. Phys. Chem. C 2017, 121, 14688−14702

(57) Guha, S.; Goodson, F. S.; Corson, L. J.; Gravenmier, C. A.; Saha, S. Boundaries of Anion/Naphthalenediimide Interactions: From Anion−π Interactions to Anion-Induced Charge-Transfer and Electron-Transfer Phenomena. *J. Am. Chem. Soc.* **2012**, *134*, 13679−13691.
(58) Shim, H.-K.; Ahn, T.; Song, S. Y. Synthesis and LED Device Properties of Carbazole and Naphthalene Contained Conjugated Polymers. *Thin Solid Films* **2002**, *417*, 7−13.
(59) Mitra, P.; Biswas, M. Synthesis and Evaluation of a Polyimide Containing Carbazole and Naphthalene Moiety. *J. Polym. Sci., Part A: Polym. Chem.* **1990**, *28*, 3795−3800.
(60) Kozycz, L. M.; Gao, D.; Tilley, A. J.; Seferos, D. S. One Donor−Two Acceptor (D−A1)-(D−A2) Random Terpolymers Containing Perylene Diimide, Naphthalene Diimide, and Carbazole Units. *J. Polym. Sci., Part A: Polym. Chem.* **2014**, *52*, 3337−3345.
(61) Lav, T.-X.; Tran-Van, F.; Bonnet, J.-P.; Chevrot, C.; Peralta, S.; Teyssié, D.; Grazulevicius, J. V. P N Dopable Semi-Interpenetrating Polymer Networks. *J. Solid State Electrochem.* **2007**, *11*, 859−866.
(62) Fulghum, T.; Karim, S. M. A.; Baba, A.; Taranekar, P.; Nakai, T.; Masuda, T.; Advincula, R. C, Conjugated Poly(phenylacetylene) Films Cross-Linked with Electropolymerized Polycarbazole Precursors. *Macromolecules* **2006**, *39*, 1467−1473.
(63) Ravindranath, R.; Ajikumar, P. K.; Bahulayan, S.; Hanafiah, N. B. M.; Baba, A.; Advincula, R. C.; Knoll, W.; Valiyaveettil, S. Ultrathin Conjugated Polymer Network Films of Carbazole Functionalized Poly(p-Phenylenes) via Electropolymerization. *J. Phys. Chem. B* **2007**, *111*, 6336−6343.
(64) Reig, M.; Puigdollers, J.; Velasco, D. Molecular order of air-stable p-type organic thin-film transistors by tuning the extension of the π-conjugated core: the cases of indolo[3,2-b]carbazole and triindole semiconductors. *J. Mater. Chem. C* **2015**, *3*, 506−513.
(65) Huang, Z.; Liu, B.; He, Y.; Yan, X.; Yang, X.; Xu, X.; Zhou, G.; Ren, Y.; Wu, Z. Facilitating triplet energy-transfer in polymetallayne-based phosphorescent polymers with iridium(III) units and the great potential in achieving high electroluminescent performances. *J. Organomet. Chem.* **2015**, *794*, 1−10.
(66) Castex, M. C.; Olivero, C.; Pichler, G.; Ades, D.; Siove, A. Fluorescence, room temperature phosphorescence and photodegradation of carbazole compounds in irradiated poly(methyl methacrylate) matrices. *Synth. Met.* **2006**, *156*, 699−704.
(67) Kawakubo, T. On the Emission of Naphthalene and Some of its Derivatives in the Crystalline State. *Mol. Cryst. Liq. Cryst.* **1972**, *16*, 333−353.
(68) Krotkus, S.; Kazlauskas, K.; Miasojedovas, A.; Gruodis, A.; Tomkeviciene, A.; Grazulevicius, J. V.; Jursenas, S. Pyrenyl-Functionalized Fluorene and Carbazole Derivatives as Blue Light Emitters. *J. Phys. Chem. C* **2012**, *116*, 7561−7572.
(69) Lee, L.; Leroux, Y. R.; Hapiot, P.; Downard, A. J. Amine-Terminated Monolayers on Carbon: Preparation, Characterization, and Coupling Reactions. *Langmuir* **2015**, *31*, 5071−5077.
(70) Morin, J.-F.; Leclerc, M. 2,7-Carbazole-Based Conjugated Polymers for Blue, Green, and Red Light Emission. *Macromolecules* **2002**, *35*, 8413−8417.
(71) Denisevich, P.; Willman, K. W.; Murray, R. W. Unidirectional Current Flow and Charge State Trapping at Redox Polymer Interfaces on Bilayer Electrodes: Principles, Experimental Demonstration, and Theory. *J. Am. Chem. Soc.* **1981**, *103*, 4727−4737.

DOI: 10.1021/acs.jpcc.7b04288
J. Phys. Chem. C 2017, 121, 14688−14702